Solar Energy 206 (2020) 918–934

Contents lists available at ScienceDirect

Solar Energy

journal homepage: www.elsevier.com/locate/solener

Synthesis of improved dye-sensitized solar cell for renewable energy power generation

Jasper Ejovwokoghene Ikpesu[a,b,*], Sunny E. Iyuke[a,b], Michael Daramola[c], Okewale A. Oyetunde[d]

[a] School of Chemical and Metallurgical Engineering, University of Witwatersrand, 1 Jan Smuts Avenue, Braamfontein 2050, Private Bag 3, Johannesburg, South Africa
[b] Department of Industrial Safety and Environmental Technology, Petroleum Training Institute, P.M.B 20, Effurun, Nigeria
[c] Department of Chemical Engineering, University of Pretoria, Hatfield, Pretoria, South Africa
[d] Department of Chemical Engineering, Federal University of Petroleum Resources, Effurun, Delta State

ARTICLE INFO

Keywords:
Synthesis
DSSCs
Renewable Energy
FTO
Graphene
Photoanode

ABSTRACT

The demand for cheap and affordable cost of fabrication and increased power conversion energy of DSSC has made most researchers sought for better ways to optimize individual parts of the cell to improve its efficiency. Thus, this paper reviews different ways to synthesize and fabricate an improved DSSC for renewable energy power generation. This article reviews the various fabrication techniques of FTO in DSSCs as well as incorporation of graphene for optimization of the DSSCs. Optimization of DSSC using FTO was reviewed with the various method of fabrication (Hydrothermal methods, CVD, Sputtering and Spray pyrolysis) for an effective light harvesting. Then, we discussed the application of graphene-based material into the various parts of the photoanode (transparent conducting electrode, semiconductor layer and dye molecules) as well as the counter electrode. Incorporating graphene into the photoanode as discussed can improve the efficiency of the cell due to its unique properties leading to a better dye absorption, improved charged separation, and excellent electrical conductivity thereby resulting in improved performance of the cell. Finally, an outlook for other trends in optimizing DSSCs was provided.

1. Introduction

The rapid drain of gas and oil resources, quest for a more sustainable form of energy, and finding on solar energy has gained it much relevance in the world today, making it a hot topic for today's researchers (International Energy Agency, 2012) (Mohammad Bagher, 2015) (Bhagwat et al., 2017). As a result of the continuous increase in demands of energy from clean sources, solar cells and Photovoltaic arrays manufacturers has grown drastically over the last two decades. Photovotalics dates back from the theory explanation of the "photovoltaic effect" which was first explained by Albert Einstein in 1904 (Jayawardena et al., 2013). He pub 9lished a simple description of "light quanta" (later called "photons") which is the basis for all photovoltaic devices and in common semiconductors (John et al., 2009) (Arons and Peppard, 1965), which gave him a Nobel Prize in 1921 for this theoretical explanation. The Fig. 1 shown below shows four main categories commonly referred to as generation and it represents the different solar cells that have been developed and has evolved over the years (Jayawardena et al., 2013):

1GEN: this is the first generation of solar cells which is based on crystalline silicon technologies, both monocrystalline and polycrystalline, and on gallium arsenide (GaAs);

2GEN: this is the second-generation of solar cells which includes amorphous silicon (a-Si) and microcrystalline silicon (_c-Si) thin films solar cells, cadmium telluride/cadmium sulfide (CdTe/CdS) and copper indium gallium selenide (CIGS) solar cells;

3GEN: this is the third generation of solar cells which involves technologies based on newer compounds including nanocrystalline films, active quantum dots, tandem or stacked multilayers of inorganics based on III–V materials, such as GaAs/GaInP, organic (polymer)-based solar cells, dyed-sensitized solar cells, etc.; and

4GEN: the is the fourth generation of solar cells which is also known as "inorganics-in-organics". This generation combines the low cost/flexibility of polymer thin films with the stability of novel inorganic nanostructures such as metal nanoparticles and metal oxides or organic-based nanomaterials like carbon nanotubes, graphene and its derivatives.

A new class of advanced photovoltaics is the Dye Sensitized solar

* Corresponding author.
E-mail addresses: Jasper.ikpesu1@students.ac.za, jasper.ie70@gmail.com (J.E. Ikpesu), sunny.iyuke@wits.ac.za (S.E. Iyuke), Michael.daramola@wits.ac.za (M. Daramola).

https://doi.org/10.1016/j.solener.2020.05.002
Received 3 March 2020; Received in revised form 27 April 2020; Accepted 1 May 2020

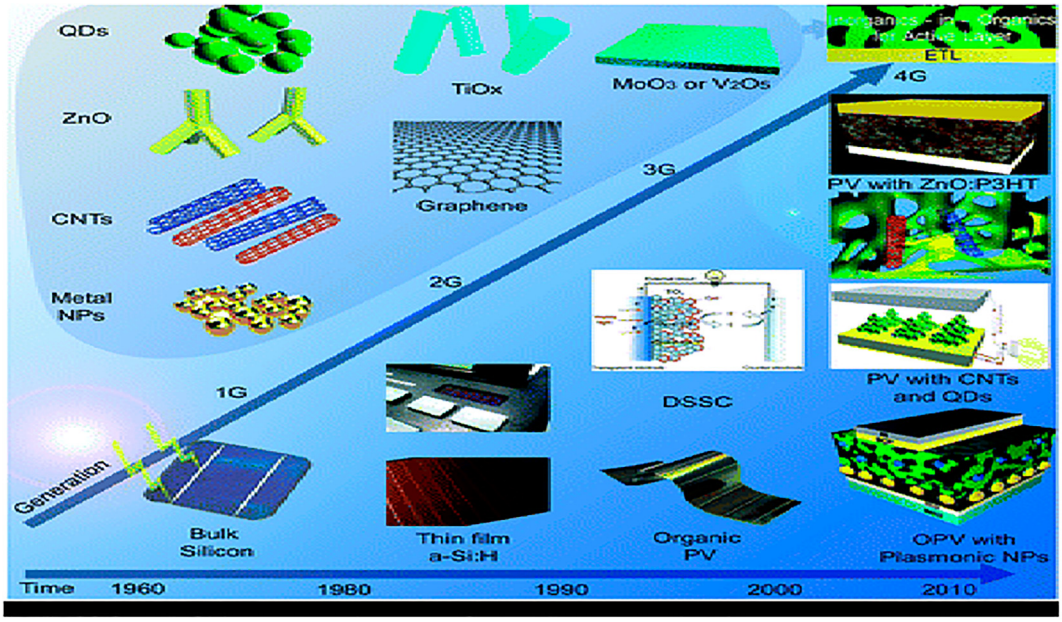

Fig. 1. The Four Generation Time line of photovoltaic associated with materials of each generation (4).

cells (DSSC). Although this class is new but it came to limelight in the third generation of photovoltaic which can be regarded as an artificial photosynthesis because of the manner in which it mimic nature's absorption of light energy from the sun and separate light absorption and charge generations (Michael, 2005). It comprises of a molecular dye, known as the sensitizer, absorbs photons and uses the energy of its own excited electrons to excite electrons to the TiO_2semiconductor. DSSC invented by Prof. Michael Gräetzel and Dr. Brian O'Regan in 1991 offers the prospect of very low fabrication cost compared to previous generations which depends on silicon based p-n junction solar cells, which require large wafers of high purity, high crystallinity silicon that are both costly and energy intensive to produce (Green, 2001). The ease of production through roll-to-roll processing and adapting of existing printing techniques provides further possibilities to reduce costs in manufacturing compared to silicon photovoltaics, which rely on batch production methods (Shah et al., 1999). Other benefits of DSSCs include their aesthetic appeal due to their partial transparency and colour, easy integration into building architecture and short energy payback time, which is the time required to generate such quantity of energy equal to the energy embodied within the system during production (Wang and Su, 2015). The efficiency of conversion of the cell is not up to the best thin-film cells. However, theoretically, the price/performance ratio should be such that it high and have capability to compete with other forms of electrical energy generation by achieving grid parity.

The need for a simple manufactured low cost photovoltaics that is efficient and fabricated with excess of non-toxic materials has led to some modification of the original DSSC design of Dr Michael Gräetzel. This has resulted to progress in the DSSC technology thus giving the technology a commercial market advantage. For over twenty-five years since the breakthrough discovery of DSSCs, numerous and positive efforts have been made on how to improve the DSSCs performance. Gräetzel (2003) reported that several different methods to how DSSCs efficiency can be improved upon, such as the use of 1-D or 3-D nanostructures of TiO_2, novel organic and natural sensitizers, alternative flexible substrates, a quasi-solid state electrolyte, or an inexpensive catalyst for the counter electrode. However, the effect of improving a single part on a whole system must be put into consideration (Khamwannah, 2015). For example, it has to be realized that the performance of the photo-anode can only be improved when done in parallel with a suitable redox couple and counter electrodes. Graphene is the most promising candidate in carbon materials for the improvement of DSSCs' performance.

Graphene has been featured in all components of the device including photoanode, dye sensitizer, transparent electrode, electrolyte and counter electrode owing to its unique and excellent proprieties. Graphene is a two-dimensional (2D) carbon element that exhibits some special characteristics ranging from excellent transmittance, high carrier mobility, and large specific surface area. For example, monolayer graphene has a high carrier mobility (greater than200 000 cm^{-2} V^{-1} s^{-1} at an electron density of $4 \times 109\ cm^{-2}$), high specific surface area ($2600\ m^{-2}\ g^{-1}$) and high optical transparency (97.7%) (Du et al., 2008); (Nair et al., 2008) and (Du et al., 2010). Over the past few years, different approaches have been explored to have incorporated graphene derivatives into various structures of the photoanode which have demonstrated different efficiency enhancements (Batmunkh et al., 2016).

The efficiencies of the graphene-based DSSCs are reportedly influenced by several factors with the most challenging task to directly incorporate graphene into structure of TiO_2 (Rho et al., 2017). Moreover, it remains an issue to industrially mass produce a graphene that is of high-quality with low cost for DSSC as photoanodes (Bonaccorso et al., 2012). When seeking for the improvement of the DSSCs, one should understand the crucial phenomena in the cell. Hence, this study presents an outlook for the synthesis and fabrication of an improved DSSCs with FTO, graphene-incorporated photoanodes and counter electrode in DSSCs, design and method of incorporation, current issues, and the research directions on the new design and innovations.

2. Structure and working principle of a DSSCs

2.1. The structural parts of DSSCs

DSSCs as illustrated in Fig. 2, comprises mainly of five parts which include a substrate, photoelectrode, sensitizing dye, electrolyte and counter electrode.

2.1.1. Substrates

The standard electrode used in DSSCs are made from conducting oxides that are transparent (commonly referred to as transparent conducting oxides (TCO)) that is coated with substrates of glass in which it is assembled to. TCOs are mostly utilized in DSSCs due to low cost, abundance, and good optical transparency within the solar spectrum that is visible and the infrared region (Khamwannah, 2015). In other to

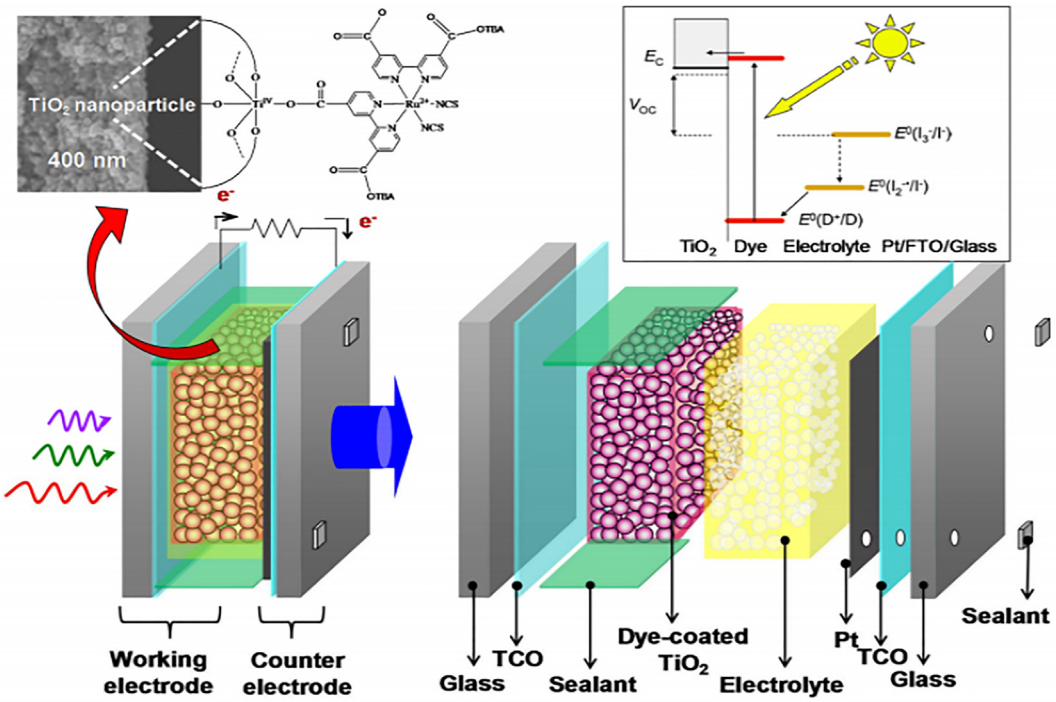

Fig. 2. Schematic Description of DSSC (Khamwannah, 2015).

make the TCO which is made from bare glass electrically conductive, a metal oxide (commonly fluorine-doped tin oxide-FTO (SnO_2F, FTO) and indium tin oxide-ITO (In_2O_3: Sn, ITO)) is used to coat it by doping. At higher temperature of about 450–500 °C during standard preparation procedure of the nanostructure and in other for thermal stability to be attained, the FTO is generally used instead of the ITO (Brian O'regan and Michael Gratze., 1991).

2.1.2. Photoelctrode

The Photoelectrode (photoanode) are made from a thin layer of sensitized wide-band gap nanostructured metal oxide semiconductor (MOS) (typically TiO_2, ZnO, SnO_2 and Sb_2O_5) deposited onto t

he TCO substrate. In order to achieve high light-harvesting efficiency (LHE), the nanostructured metal oxide semiconductor layer must provide a large surface area (high roughness) to permit the adsorption of a large amount of sensitizer molecules (Brian O'regan and Michael Gratze., 1991) and (Nazeeruddin et al., 1993).

2.1.3. Dye molecules (photosensitizers)

The photosensitizer is of utmost importance in the functioning of a DSSC as they play a vital role in sensitizing the wide-bandgap of a nanostructured photo electrode and has, therefore, been a topic of interest for researchers over the years with hundreds of different dyes being tested. In a more ideal case, an effective sensitizer should provide high light absorption in the whole visible region of the solar spectrum and also into the Infrared region to maximize light harvesting. It should feature a suitable anchoring group, such as a carboxylic acid, by which it can be attached to the semiconducting oxide (Miles, 2015).

2.1.4. Redox electrolyte

The electrolytes widely used in typical DSSCs are formed of a redox couple ($I-/I3-$) dissolved in a suitable solvent typically acetonitrile (ACN) and, typically, some additives to boost the cell performance (Gratzel, 2003) and (Miles, 2015). In DSSC, the electrolyte is needed for dye regeneration and to complete the electron transportation in between the photo electrode and counter electrode. The choice of solvent used in the electrolyte is impactful and there are several research carried out on different type of solvents for the electrolyte, such as alcohols, propylene carbonate, γ-butyrolactone, tetrahydrofuran, N, N-dimethylformamide (Hara et al., 2001); (Naohiko et al., 2009) and (ChunHung et al., 2010), as well as different types of nitrile solvent (Ze et al., 2011).

2.1.5. Counter electrode

The Counter electrode (CE) is a very vital part in the DSSC and its role is to reduce the materials involve in redox reaction, which are the mediators for regenerating the sensitizer (dye) after electron injection (Gratzel, 2003). When the dye molecules are regenerated, it produces triiodine which will be reduced to iodide ion at counter electrode. Generally, a DSSC counter electrode is prepared from a small amount of platinum (Pt) catalyst deposited onto a TCO glass. Platinum is a widely used CE material as result of its high catalytic activity and stability toward the iodide electrolyte (Papageorgiou et al., 1997); (Xiaoming et al., 2004) and (Seok-Soon et al., 2006). Despite the wide usage of Pt as counter electrode, (Bhagwat et al., 2017) found out that the stability of FTO-based Pt varied with method of preparation as a result of generation of PtI_4 due to corrosion by triiodide solutions. This and its limited availability made several researchers seek an alternative with nickel.

2.2. Working principle of a DSSCs

DSSC operates with the principle of absorption, separation and collection (Muhammad, 2017) with the absorption of light and the transportation of charges constituting the two major ways in which the DSSCs differ from all other solar cells (Eran et al., 2011). The dye molecule which is an important part of the cell that coats the semiconductor support, absorbs light and excites the electron from the highest occupied molecular orbital (HOMO) to the lowest unoccupied molecular orbital (LUMO) thereby producing a combination of an excited electron and an electron hole which is known as an exciton. The HOMO is the part of the cell that has the lowest energy level of the cell while the LUMO has the highest energy level of the cell as shown in Fig. 2.

The absorption of light is then followed with separation which it involves the injection of exciton into the conduction band of metal

oxide semiconductors (MOS) and the dye molecule being oxidized. In order for current to be produced, the two opposite charges must be separated at the interface of MOS and the dye thereby preventing them from recombining. When these charges are produced, the excited electron is transported through a semiconductor support medium to the anode while the excited holes are transported through the electrolyte on the opposite side of the dye to the cathode (Miles, 2015). After this is done, the circuit is completed and the electrons are made to pass around the circuit by the light absorbing dye molecules (Archer and Nozik, 2008).

In all solar cell designs, it is important that one of the electrodes in use must be made from a conducting material that is transparent commonly known as TCM, such as FTO, in order to permit the transmission of light to the dye molecules (Miles, 2015) while the materials to be used for the other electrode can vary depending on the cell design and can be chosen to either transmit light or reflect light back towards the sensitizer to increase light absorption. In the commonly used cell design, developed by Grätzel in 1991, a sensitizer is adsorbed onto a high surface area semiconductor consisting of a mesoporous film of titania nanoparticles. The liquid electrolyte contains a redox mediator, typically the I-/I3- redox couple, which is regenerated at the platinum coated counter electrode.

All of the components within the cell need to be carefully selected in order to correctly

align their respective energy levels as shown in Fig. 3. The maximum output voltage (V_{oc}) of the cell is ultimately resolved by the difference in potentials between the conduction band edge of the semiconductor support and the redox potential of the electrolyte. These potentials therefore need to be matched as closely as possible to the LUMO and HOMO levels of the dye in order to minimize energy losses (Archer and Nozik, 2008) (see Fig. 4).

2.3. Chemical reaction in a DSSC

The chemical reaction involves in a DSSC working principles are categorized into six major reactions which includes absorption reaction, electron injection, electron transport, triiodide reduction, regeneration of dye and the recombination process as shown in Fig. 3. The recombination processes decrease the efficiency of the DSSC and result to energy losses.

The first reaction that takes place in the DSSC when struck by light and photons is absorption of dye molecules because of an excitation that exists between their electronic states. The excitation is naturally a metal-to-ligand charge transfer (MLCT) (Anwar, 2013) and it tends to

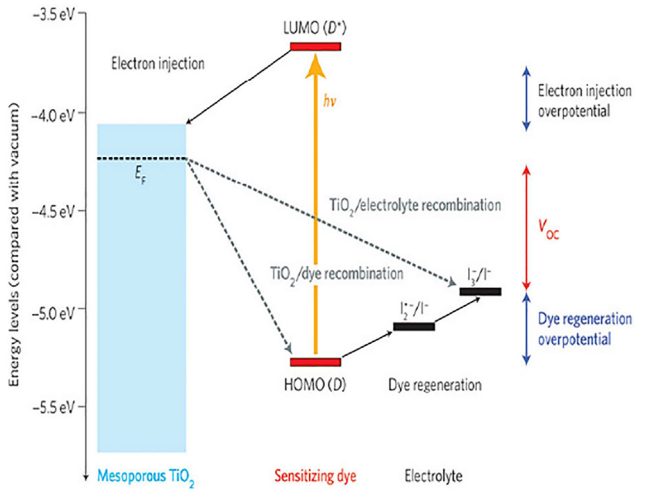

Fig. 3. The Working Principle of a Schematic of DSSCs (Mohammad Bagher, 2015).

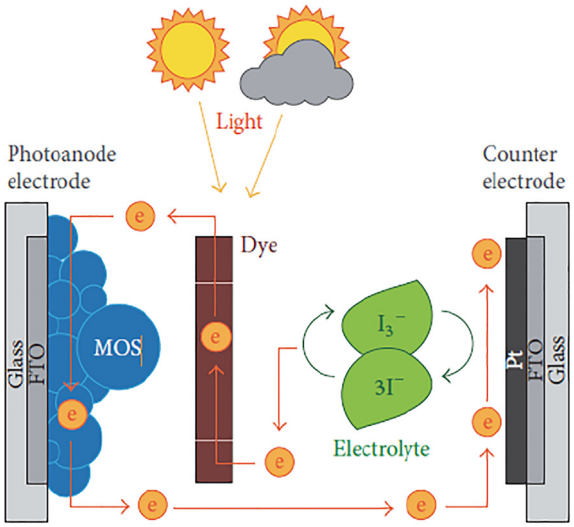

Fig. 4. Schematic structure of DSSC (Ahmad et al., 2017b).

cause electrons to move from the HOMO level to the LUMO level of the molecular ground state (van de Lagemaat and Frank, 2000). The absorption state is also known as the excitation state as shown in equation (1) below

$$S + \text{photon} \rightarrow S^* \quad (1)$$

After Absorption of light occurs and excitation has taken place, electron in injected metal oxide semiconductor conducting band is made up of TiO_2 as shown in equation (2).

$$S* + TiO_2 \rightarrow e - (TiO_2) + S^+ \quad (2)$$

The movement of the electrons happens as a result of diffusion that occurs from the electronic concentration gradient in nanoporous TiO_2 (Soedergren et al., 1994) and (van de Lagemaat and Frank, 2000) while other studies also showed that these movement is due to the incident light intensity (Sulaeman and Abdullah, 2017). The coefficient of diffusion of the electrons is dependent on the quasi-Fermi level under illumination of the electron (Soedergren et al., 1994) and these reports were explained using a multiple trapping (MT) model (Fisher et al., 2000); (Bisquert et al., 2004) and (Bisquert and Vikhrenko, 2004). The collection of charges in DSSCs, is due to the kinetic competition in between the movement of the injected electrons in the nanoporous semiconductor layer and the recombination reaction of these electrons with the redox species in electrolyte or with the oxidized dye molecules (Anwar, 2013). For the charges to be collected efficiently, the movement of electron must be much faster than recombination and this must be done within order of milliseconds (Peter and Wijayantha, 2000) and (Frank et al., 2004).

$$e^-(TiO_2) + CE \rightarrow TiO_2 + e^-CE + \text{electricity energy} \quad (3)$$

The triiodide reduction to iodide in DSSCs happens at the counter electrode and it is the fourth stage in the cycle of DSSCs reaction. In order to increase the performance of DSSCs, the catalytic activity of the counter electrode must be high for this reaction in order to reduce the energy loss. The most commonly used catalyst in the counter electrode is the Platinum (Pt) because of its high catalytic activity for triiodide reduction (Anwar, 2013) as shown in the equation (4) below.

$$I_3^- + 2e^-(CE) \rightarrow 3I^- + CE \quad (4)$$

This is the fifth energy reaction in the DSSC and it involves the regeneration of dye. The electrolyte used in DSSCs is usually gotten from an organic solvent having the I-/I3- redox couple that plays an important role in the fourth and fifth reaction.

$$S^+ + 3I^- \rightarrow 2S + I_3^- \quad (5)$$

The recombination process involves a series of energy reactions divided into three step reaction process. There is a possibility that electrons in the TiO_2nanoporous film can recombine with either oxidized dye molecules or triiodide in the electrolyte as these electrons are always within a few nanometers distance of the semiconductor/electrolyte interface.

The first stage of this recombination process is a very slow reaction as compared to electron injection in TiO_2 as shown in equation (6). The next reaction is a recombination of injected electrons in the TiO_2 with the triiodide ion at the interface, also known as dark current, is one of the undesirable processes in the DSSC as shown in equation (7). This process is much more probable than the initial process reaction (Gratzel et al., 2008). The final reaction of recombination could also occur on the transparent conducting oxide (TCO) as the TiO_2 film may not fully cover the TCO as shown in equation (8). However, researches have shown that this effect is small and negligible as platinum-free TCO has very poor electrocatalytic activity towards the iodine/triiodide redox system (Cahen et al., 2000). The first stage of the recombination reaction process must proceed slowly as compared to the electron injection and regeneration of dyes in order to have significant charge separation hence the kinetics of this reaction follows a multi-exponential time law, taking place on a microsecond to millisecond time scale as compared to ultrafast electron injection (Haque et al., 2000) and (Kuciauskas et al., 2000). It depends on the density of electrons in the semiconductor and the intensity of light (Anwar, 2013).

$$e^- (TiO_2) + S^+ \rightarrow S^0 \quad (6)$$

$$2e^- (TiO_2) + \Gamma_3 \rightarrow 3\Gamma \quad (7)$$

$$2e^- (TCO) + \Gamma_3 \rightarrow 3\Gamma \quad (8)$$

2.4. Effectiveness of an optimized DSSC

Several studies have been carried out on how to effectively optimize the DSSC for optimum performance. They are basically focused on modifying the structures and major parts of the (Eran et al., 2011), in his research state that there is a significant difference between the size of solar cells studied in a research laboratory and those that are actually applicable on a large scale. Meanwhile in 2007, Lenzmann and Kroon studied the effect of DSSC size without considering stability, and found that efficiency decreased with DSSC size (Lenzmann and Kroon, 2007).

The glass used for DSSCs is made to be conductive in order to facilitate the collection of free electrons produced and help transfer the current out of the cell. Since the glass plates are the outer boundaries of the cell, any incoming light must travel through the glass. Thus, the optical properties of the glass are critical to the cells functioning (Eran et al., 2011). The glass must be highly transparent in the absorbing region of the sensitizers in order to excite electrons within the DSSC.

Kay and Gratzel (Kay and Gratzel, 1996) described the photoelectrode of the DSSC as a conductive glass plate "coated with a porous layer of a wide band gap semiconductor, usually TiO_2, which is sensitized for visible light by an absorbed sensitizer (Kay and Gratzel, 1996). They applied colloid TiO_2 by the doctor-blading method (using a rod pressed against the surface to spread across the surface) to the conductive side of glass with SnO_2 film. Then, the glass coated in TiO_2 was heated to 450 °C (Kay and Gratzel, 1996). Next, the glass coated in TiO_2 was soaked in sensitizing dye to complete the photoelectrode. This process is standard to most DSSCs. As revealed by an extensive literature review, there have been very few changes to the semiconductor in the last fifteen years. Most experiments affecting the photoelectrode have dealt with changing the sensitizer of the electrode: the dye (Eran et al., 2011). Otherwise, the main developments in the photoelectrode have only involved the use of different types of TiO_2.

TiO_2 has been used as the semiconductor in DSSCs since their inception because of its low cost, excellent semiconducting properties, and already widespread use as a white colorant in toothpastes and paints (Kay and Gratzel, 1996). Different types of TiO_2 can affect the abilities of a cell. Kang et al., (Kang et al., 2008) recommended using TiO_2nanorods instead of TiO_2 nanoparticles. Nanorods result in improved charge transport, and induce a longer lifetime for the electron in the photoelectrode due to necking of the rods in a unique 3D network (Kang et al., 2008). As a result of the increment of the area of the surface of nanorods over nanoparticles, the initial conversion efficiency of nanorod based DSSCs is 3.32% compared to that of nanoparticle-based DSSCs at 1.97%. Nanorod-based DSSCs also have higher overall conversion efficiency in an environment of increasing salt concentration. The conversion efficiency of nanorod based DSSCs remained constant while the conversion efficiency of nanoparticle-based DSSCs decreased with increasing salt concentrations. These results led to the conclusion that nanorod-based DSSCs performed better in extreme environments and overall than nanoparticle-based DSSCs.

Over the years, the study of graphene has brought so much interest to researchers due to carbons unique characteristics of bonding with other element easily. In a study conducted out by Long et al., (Long et al., 2012) on the composites of graphene/TiO_2, they found out that graphene has an outstanding potential for photovoltaic uses, which provided an efficient photo induced charge separation at the interface (Long et al., 2012). Jang et al., (Jang et al., 2015) incorporated graphene into a TiO_2 using the modified Hummer's method and the result showed that the PCE was improved by 47% when compared to a pure TiO_2 (Jang et al., 2015).

The redox couple is the key component to the effectiveness of DSSCs (Boschloo and Hagfeldt, 2009) where iodide (I-) reduces the dye molecules that has been oxidized by the incoming photon and becomes triiodide (I3-) and the triiodide moves to the counter electrode and is reduced back into iodide. The iodide can then reduce the dye that has been newly oxidized by the second incoming photon. This cycle keeps occurring, depending on the redox reactions occurring with the redox couple mediator (I-/I3-) (Eran et al., 2011). According to Boschloo and Hagfeldt (Boschloo and Hagfeldt, 2009) in their review of the iodide/triiodide redox mediator, "the photovoltage of the device depends on the redox couple because it sets the electrochemical potential at the counter electrode." Kinetically, this is because the "driving force for dye regeneration reaction is given by the difference between" the energy states of the standard dye with the oxidized dye and iodide with diiodide (I2-) (Boschloo and Hagfeldt, 2009).

3. Optimization of DSSC using FTO

Transparent conductive materials (TCMs) are generally from a category of materials that tends to have both electrical conductivity and optical transmission simultaneously. Generally, they are thin films in form which range from metal films, wide-band-gap semiconductors, metal nitrides or doped organic polymers (Zhang et al., 2014) and are predominantly in use when considering solar cells (Granqvist, 2007) and (Ginley et al., 2010). The fluorine-doped tin or tin-doped indium oxide (FTO or ITO) are most commonly used TCO because it can make the glass plates serve as electrodes helping them to collect electric charge produced within the cell. Their coatings of both the FTO and ITO are very transparent throughout the visible spectrum and they are more absorbent in ranges closer to UV radiation, making them well suited for the main part of the Sun's output (Longo and Paoli, 2003). Both FTO and ITO coatings share a typical resistivity of between 10 and 20 Ω/cm^2. However, the resistivity of glass-ITO electrodes increases significantly as temperature rises and this effect is not observed in FTO covered glass (Longo and Paoli, 2003).

FTO can be mechanically, chemically and electrochemically stable utilizing numerous technologies other than solar cells. There are several methods used in fabricating the FTO nanocomposites which includes the hydrothermal method, chemical vapour deposition (CVD), RF sputtering and spray pyrolysis method.

3.1. Hydrothermal method

This method is often one of the very best when considering cost and prospect as it is capable of preparing a thin film of FTO that is homogeneous. This is a process that involves deposition of liquid as it has to do with bottom-up approach (which is also called soft chemistry) thus resulting to a thin film which is homogeneous also having stable pressure and temperature (Ahmad et al., 2017a). Water is referred to as a universal solvent due to its nature, high importance and outstanding characteristics (Muhammad, 2017) and this method utilizes this as a reaction medium. It is a medium for reaction which happens in totally different hydrothermal conditions when compared to standard conditions. The most important advantage of using are basically the benefits it has environmentally (i.e. water being the most effective solvent when it comes to cost and acting as a catalyst for the formation of desired materials). It has no toxic effect, does not cause fire or explosion, noncarcinogenic, nonmutagenic and thermodynamically stable (Muhammad, 2017). Water has high volatility thus making it very easy to taken out of any process.

Relatively, the nanostructure of FTO are affected by the method itself and also by the parameters of the experiment (Sasha et al., 2015). In other researches, the method that is solution-based method was seen to give low cost of production with a high growth rate of seed layer that is simple on the nanostructured FTO when compared to the amorphous method (Sasha et al., 2015). For example, the hydrothermal process of growing ZnO nanostructures has gathered immense popularity as a result of the simplicity and conditions of growth tolerable (Suhaimi, 2015). In 2009, Liu and Aydil discovered a hydrothermal method that was simple. The method was used for growing oriented single crystalline rutile TiO_2 nanorods on FTO substrates (Liu and Aydil, 2009). When these methods were compared to other methods, hydrothermal method gained prospect for the fabrication of nanostructured FTO thin film. Over the last 20 years, different nanostructure of FTOs had been reported such as nanobows, nanocages, nanorods and nanobelts which showed different characteristics (Sasha et al., 2015).

In a study conducted by Sasha et al., (Sasha et al., 2015) on the preparation of a nanostructured FTO using the hydrothermal process, nanostructure was directly synthesized on FTO glass substrate by using pentahydrate stannic chloride ($SnCl_4{\cdot}5H_2O$) and ammonium fluoride (NH_4F) as precursors (Sasha et al., 2015). During the synthesizing process, different application of variation of time was applied and the characteristics of nanostructured FTO were investigated via field emission scanning electron microscopy (FESEM). The FESEM images revealed the growth of nano-sized particles layer on the FTO substrate. The electrical properties studied have shown a degeneration of conductivity as the thickness of nanostructured layer increased. UV–Vis results showed the decrement of transmittance as the time duration increased. It was revealed through FESEM characterization that the nanostructured FTO can be improved by using dibutyltindiacetate (DBTA) as a precursor (Sasha et al., 2015).

3.2. Chemical vapor deposition (CVD)

The preparation of FTO by CVD has different variations which includes low pressure CVD plasma enhanced CVD (Jubault et al., 2007) and the atmospheric pressure CVD which is very productive and economic (Yang et al., 2010) and (Wang et al., 2015).

Najafi and Rozati (Najafi and Rozati, 2017) used the atmospheric pressure CVD method to prepare FTO by depositing it onto a glass substrate at different substrate temperature and were later kept constant at 500 °C using air as both the career gas and the oxidizing agent (Najafi and Rozati, 2017). Investigating the electrical properties of the prepared thin film showed that its properties tends to vary with the varying substrate temperatures ranging from an insulator thin film to a highly conductive thin film (Najafi and Rozati, 2017). Under X-ray diffraction, the structural property was seen to be poly-crystalline at higher temperatures and amorphous at lower temperature.

3.3. Sputtering

In order to deposit the thin film effectively, some techniques used in preparing FTO require high substance substrate temperature and also post-treatment such as annealing leading to the formation of intermediate semiconductor oxide layers at the film boundary and additional operational cost respectively (Banyamin et al., 2014). Over the years few attempts has been made to use sputtering to prepare FTO compared to other methods. This method poses to be environmentally friendly and the use of loosely packed blended powder targets gives an efficient means of screening candidate compositions, which also provides low cost of operation (Banyamin et al., 2014). This methods dates back to 1955 when it was used to produce a small grain size of In_2O_3:Sn (Muhammad, 2017). The magnetron sputtering is the only technique suitable for high quality for large scale deposition, well adhered and large sized films at relatively low substrate temperatures (Zhu et al., 2017). There are different sputtering method which includes the direct current (DC) reactive sputtering method (Liao et al., 2011); (Liao et al., 2014) and (Jager et al., 2014) and the radio frequency (RF) sputtering (Maruyama and Akagi, 1996); (de Moure-Flores et al., 2013) and (Zhu et al., 2017).

The introduction of hydrogen into sputtering atmosphere has shown theoretically in calculations that hydrogen can act as a source of n-type conductions in ZnO materials (Cox et al., 2001); (Lavrov et al., 2005) ; (Janotti and Van de Walle, 2007) and (Van de Walle, 2012) (xxxx). However little research has been carried out to justify the claim that hydrogen can be introduced to the sputtering atmosphere of SnO_2 since it is most widely used. Liao et al., (Liao et al., 2011) attempted to introduce H_2 into the sputtering atmosphere in order to improve the conductive property of the film (Jager et al., 2014). While in 2013, de Moure-Flores *et al.,* also tried to optimized a SnO_2-based film by introducing the same hydrogen into the sputtering atmosphere (Zhu et al., 2017). In the research, FTO films was deposited by the RF sputtering method with SnO_2- SnF_2 target as fixed H_2/Ar concentration ratio of (3/97) and effect of H_2 concentration in the sputtering atmosphere was investigated and more research are still been done.

In 2017, Zhu *et al.,* prepared a thin film of FTO using the sputtering SnO_2- SnF_2 target introduced by de Moure-Flores *et al.,* in 2013 in a similar H_2/Ar atmosphere in order to investigate the H_2/Ar flow ratio on the properties of the film at two different substrate temperature (Zhu et al., 2017) and (de Moure-Flores et al., 2013). Zhu et al., (Zhu et al., 2017) found out that introducing H_2 can lead to formation of FTO thin film with a (1 0 1) Ar flow ratios in the film and that resistivity of film tends to decrease at first and later increases above a certain value (Zhu et al., 2017). The increase of H_2/Ar flow rate result to a decrease in the conductivity, transmittance and the band gap (Zhu et al., 2017).

In a research carried out by Zaid *et al.,* (2014), FTO were produced from blended SnO_2 and SnF_2 powder after which the fluorine doping level was investigate (Banyamin et al., 2014). During the investigation at different doping level, different film thickness was obtained with their subsequent electrical and optical properties. The result depicted that the optimized conditions of a thin film of an average visible transmittance of 83% and optical band-gap of 3.80 eV, resistivity of $6.71x10^{-3}$ cm^{-3} and a mobility of 15 cm^2/Vs.

3.4. Spray pyrolysis

The use of spray pyrolysis to make TCO dates back to 1947 when Mochel (Mochel, 1947) incorporated Sb to SnO_2 and McMaster (Mcmaster, 1947) incorporated Cl to SnO_2. Over the years it has been deployed to various TCO which includes doping tin oxide with fluorine (FTO) (Mochel, 1947) and (Mcmaster, 1947). Spray pyrolysis is a widely used method because of its simplicity, low cost of experimental apparatus, ready incomparability of various dopants, high growth rate

and high mass production compatibility for large area coating (Aouaj M. A.; Diaz R.; Belayachi A.; Rueda F.; Abd-Lefdil M. (2009). Comparative Study of ITO and FTO Thin Films Grown by Spray Pyrolysis. Mater. Res. Bull, 44(7), 1458–1461. Bagher A. M., Mirzaei M. A., Mohsen M, 2015). This is a process in which a thin film of required material is deposited on to a hot surface by spraying a precursor solution on to it. Several tin compounds have been used as a tin element in the precursor solution for preparing FTO films. Their preferred crystal growth orientation and crystal size differs with the nature of the compound used which in turn affects the optical and electrical properties as well as the conductivity (Napi Mohd et al., 2016).

In a research conducted by Murakami (2007), he observed an initial growth of the SnO_2 on the glass substrate. He found out that each isolated grain had grown almost at similar rate in which its density had increased with the surface area roughness during the initial stage. He observed that an increase in roughness would lead to a relative spread of the grain (Murakami et al., 2007). However, in 2013, Liyanage *et al.* was able to improve the spray pyrolysis to get nanorods films made of FTO that has a low resistance sheet property (Liyanage, 2013). In the improved spray pyrolysis, a horizontal method of spray was used to keep the pressure low during deposition process and maintaining a good percentage of transmittance of FTO films.

The size of grain of FTO films was found to be dependent on the temperature in which deposition occurs; the time at which reaction happen; the type of precursor and solvent that were used (Muhammad, 2017). Mohalkar *et al.,* (2008) also investigated the effect of various solvents used for FTO films fabrication and he found out that various type of solvents used in the fabrication of FTO films would be able to get a new morphology of FTO films without affecting the lattice parameter values (Moholkar et al., 2008). However, in 1998, Smith *et al.,* proposed different type of FTO film morphologies which were dependent on the precursor and solvents pairs (Smith, 1995). From the pairing of solvent and precursor, the obtained films layers have been classified into three categories which were smooth, slightly faceted and faceted surfaces (Muhammad, 2017).

In a quest to optimize the performance the FTO, Hassanien *et al.,* (2015) prepared thin films of undoped SnO_2 and fluorine doped tin oxide (FTO) using the spray pyrolysis on glass substrates while a systematic optimization of the solvent and precursor was investigated (Hussein et al., 2016). Hassanien *et al.,* (2015) found out that when the spray time, the temperature of the substrate and solution concentrations were increased, it resulted in subsequent increase in film thickness and a decrease in sheet resistance (Hussein et al., 2016). This invariably means that as thickness of film is achieved, growth rate of SnO_2 is optimized. The electrical and optical properties of FTO are essential both for effective light harvesting and sheet resistance. Hassanien *et al.,* (2015) observed that the electrical resistance of the film is thickness dependent and as such, the increased thickness as a result of the increase in spray time, substrate temperature and solution concentration led to a decrease in the sheet resistance thereby enhancing the conductivity (Hussein et al., 2016).

In 2016, Napi *et al.* prepared FTO using Ammonium Fluoride and DBTDA by mixing the two solutions and then spray pyrolysis method was adopted to produce the FTO substrate (Napi Mohd et al., 2016). The research focused on varying the anneal temperature of the sample. Napi *et al.,* (2016) observed that by adjusting the anneal temperature, the best film was obtained at a temperature of about 150 °C thereby producing a sheet resistance of $5.11x10^8\Omega$/sq with a highest percentage of transmittance (Napi Mohd et al., 2016). Also, it was observed that an increase in the anneal temperature resulted to an increase in the growth of the thin film because an increase in anneal temperature will result to increase in supply energy.

4. Graphene

4.1. Fundamental and characteristic properties of graphene

Fascination with graphene has been growing very rapidly in recent years and the science of graphene is now becoming one of the most interesting and fast-moving topics in material science (Aoki et al., 2014). The horizon of graphene is ever becoming wider, where physical concepts go hand in hand with advances in experimental techniques. On the other hand, graphene attributed properties such as high surface area, excellent transparency, light absorption, and charge transport properties have significantly aroused interest from different research fields concerned with energy conversion and environmental pollution remediation (Tahir et al., 2016).

Graphene is the first truly 2D crystal ever observed in nature and this is remarkable because the existence of 2D crystals has often been doubted in the past mainly due to Mermin-Wagner theorem stating that a 2D crystal loses its long-range order, and thus melts, at any small but non-zero temperature as a result of thermal fluctuations. According to Zhen and Zhu (Zhen et al., 2018), graphene is an allotrope of carbon in the form of a 2D, atomic-scale, hexagonal lattices in which one atom forms each vertex with sp^2 hybridization as shown in Fig. 5.

The unit structure of graphene is a hexagonal carbon ring with an area of 0.052 nm^2, carbon–carbon bond length is about 0.142 nm and a stable hexagonal structure is formed through strong connections by three σ bonds in each lattice (Zhen et al., 2018). In graphene, each carbon atom uses 3 of its 4 outer orbital electrons to form 3 sigma bonds 120^0 apart with 3 adjacent carbon atoms in the same plane, leaving the 4th electron free to move, therefore, electrons in graphene behave just like massless relativistic particles without crystal lattices restrictions (Wei et al., 2018) and (Li et al., 2015). As such, graphene possesses excellent electrical conductivities in two dimensions at room temperature (more than 200,000 $cm^2\ V^{-1}\ s^{-1}$) (Si and Samulski, 2008).

As a 2D material, graphene has zero band gap with a single molecular layered structure (Wei et al., 2018); the electrical conductivity of graphene is mostly attributed to the π bond located vertically to the lattice plane (Zhen et al., 2018). Graphene's stability is ascribed to its tightly packed carbon atoms and a sp^2 orbital hybridization—a combination of orbitals s, p_x, and p_y that constitute the σ-bond. The final p_z electron makes up the π-bond. The π-bonds hybridize together to form the π-band and π*-bands. These bands are responsible for most of graphene's notable electronic properties, via the half-filled band that permits free-moving electrons (Zhen et al., 2018). Moreover, graphene is known for its tranparancy in the visible region which is attributed to its extreme thinness, this is found useful in DSSC's conductive substrate (Chae et al., 2017) and (Britnell et al., 2013).

4.2. Synthesis of graphene

The elusive two-dimensional form of carbon is probably the best-studied carbon allotrope theoretically. Graphene is the starting point for all calculations on graphite, carbon nanotubes, and fullerenes; at the same time, numerous attempts to synthesise these two-dimensional atomic crystals had usually failed, ending up with nanometre-size crystallites (Oshima and Nagashima, 1997). These difficulties are not surprising in light of the common belief that truly two-dimensional crystals cannot exist (in contrast to the numerous, known quasi-two-dimensional systems). Moreover, during synthesis, any graphene nucleation sites will have very large perimeter-to-surface ratios, thus promoting collapse into other carbon allotropes. Experimental efforts to obtain graphene could be traced to Boehm et al., (Boehm et al., 1962) early work of transmission electron microscopy who found single- and few-layer graphite structures in solution, as a product of graphene oxide (GO) reduction (Boehm et al., 1962). There were renewed efforts in the 1990 s which lead to the deposition growth of graphene on metal surfaces but little success was recorded until Novoselov et al. (Novoselov

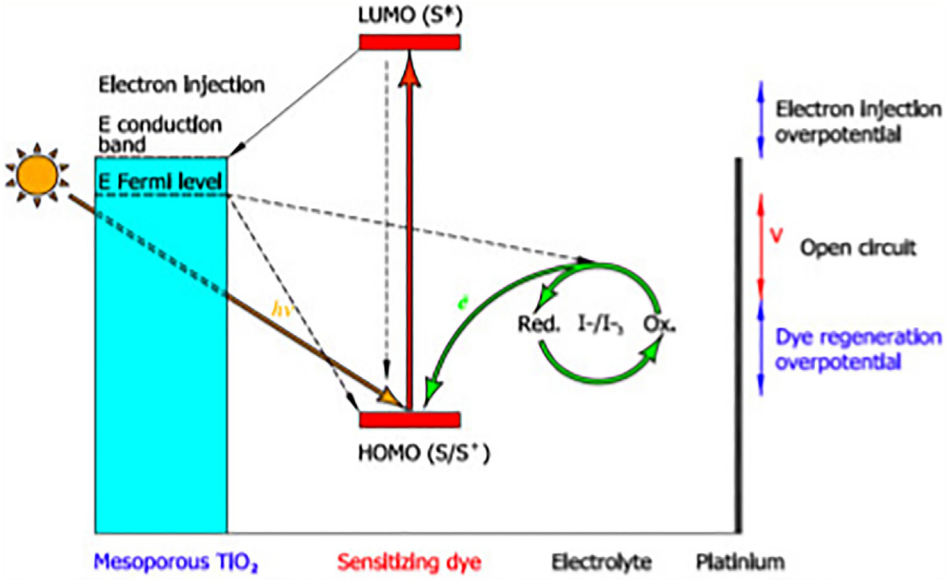

Fig. 5. Energy level diagram of DSSCs (Mahmoud et al., 2016).

et al., 2004) carried out a pioneer work to isolate graphene monolayer from highly-oriented pyrolytic graphite (HOPG) through mechanical exfoliation in 2004 using their skillful scotch-tape technique (Novoselov et al., 2004).

Ever since the first graphene isolation, several efforts have been employed to synthesise graphene. The syntheis methods are classified into two categories namely 'top-down' and 'bottom-up'. An overview of different synthesis techniques (flow chart) is presented in Fig. 6.

Development of effective approaches for graphene synthesis is of crucial importance, this depends on the purpose of application raging from the desired size, orientation, thickness, morphology, purity and efflorescence of the specific product. In top-down process, graphene or modified graphene sheets are produced by separation/exfoliation of graphite or graphite derivatives (such as graphite oxide (GO) and graphite fluoride (Bhuyan et al., 2016); (Li et al., 2014) and (Zhang et al., 2015). The most popular top-down method is via the exfoliation of graphite. One of the key challenges in this approach is aggregation while processing bulk-quantity graphene sheets which tends to form irreversible agglomerates or even restack to form graphite through Van der Waals interactions unless well separated from each other (Zhang et al., 2018).

On the other hand, the bottom-up approach starts the production of graphene from small organic molecules. This approach is notable for its precise control over the morphology and structure of graphene (Bhuyan et al., 2016). The most popular bottom-up approach seems to be chemical vapour deposition (CVD) method. Different reports have shown that graphene have been synthesised by decomposition of hydrocarbons (such as methane) into graphene which was catalysed by metal surfaces through CVD (Huilei et al., 2012). The deposition of high-quality graphene from CVD process is usually done onto various transition-metal substrates like as Ni, Pd, Ru, Ir, and Cu (Bhuyan et al., 2016). Another important method of bottom-up approach is Epitaxial thermal growth or thermal decomposition method, this method allows the growth of graphene on a single crystalline silicon carbide (SiC) surface (Zhang et al., 2014). Besides, graphene oxide reduction is known to be another way of getting graphene through Brodie method, Staudenmaier method, Hummers method (Kaiser et al., 2007) and (Nurhafizaha et al., 2017).

4.3. Multidimensional forms of graphene

Research in the field of graphene has continued to be application driven. Owing to the increasing and expanding applications of graphene in different areas, 2D graphene sheets has been tailored to obtain other dimensional forms namely one (1D) and three (3D) dimensional forms. 1D and 3D graphene-based derivatives exhibit many amazing properties, as well inherit intrinsic properties of 2D graphene and could be applied in multiple areas (Zhang et al., 2015); (Zhang et al., 2014) and (Xu et al., 2015). The synthesis of 1D graphene fibres and nanoribons has in the recent years triggered numerous research. Graphene

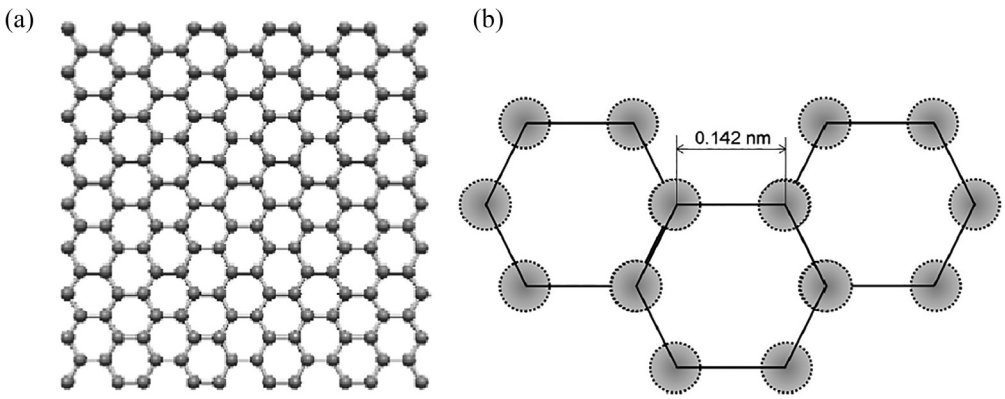

Fig. 6. (a) Two-dimensional (2D) graphene (b) Hexagonal lattice of graphene (Zhen et al., 2018).

nanoribons (GNRs) are formed by constraining large-area graphene in one dimension purposely for tuning the electronic properties of graphene for different applications and bandgap engineering, and whose properties highly depend on their size and edge shape. 1D graphene (fibers) can be prepared from graphene oxide suspensions by wet-spinning of carbon nanotubes (CNTs) (Seok-Soon et al., 2006); (Xu et al., 2013) ; (Xiang et al., 2013) and (Zhang et al., 2018), other methods include dimensionally-confined hydrothermal strategy (Luo et al., 2012) and chemical reduction (Li et al., 2014). It can also be prepared from graphene films such as chemical vapor deposition grown graphene film (Li et al., 2011) and graphene oxide film (Zou and Kim, 2012). Graphene nanoribbon can be obtained from the longitudinal unzipping of CNTs (Li et al., 2015). 1D graphene has been applied in DSSCs, used GNRs at the counter-electrode and I^-/I_3^--based electrolyte and recently incorporated GNR into TiO_2-photoanode and it was observed that the GNRs significantly improved the photoconversion efficiency (PCE) of the dye-sensitized solar cells (DSSCs) (Zou and Kim, 2012).

Part of the efforts made to diversify the graphene-based applications is the development of a graphene with band gap. What differentiates graphene quantum structures from graphene is the modification of electron behavior (i.e. graphene's physical properties) due to quantum confinement. When graphene is reduced to a size comparable to the exciton Bhor radius, quantum confinement effects become observable, the electrical and optical properties of graphene quantum structure is affected by the particular size, shape and edge structure (Li et al., 2015); (Li et al., 2014) and (Li et al., 2017). Soon Kim et al., (Kim et al., 2006) predicted an existence of bandgaps in graphene nanoribbons (GNRs). It was claimed that based on a first principles approach, a band gap exists in zigzag GNRs due to a staggered sublattice potential, while a bandgap in armchair graphene exists due to quantum confinement and edge effects (Kim et al., 2006); such predictions were then confirmed by pioneering experimental work from Chen et al., (Chen et al., 2007) and Li and Kaner, (Li and Kaner, 2008) (Chen et al., 2007) and (Li and Kaner, 2008). In 2008, Ponomarenko et al., (Ponomarenko et al., 2008) fabricated graphene dot structures with different sizes by electron beam lithography and observed quantum-induced bandgap in more strictly defined graphene quantum dot structure (Ponomarenko et al., 2008). Comparing the Coulomb blockade peaks of different structures, they observed non-periodic Coulomb blockage peaks for graphene quantum dot (GQD) sizes smaller than 100 nm, a strong indication of quantum confinement induced bandgap effects in graphene quantum dots. GQDs have been reportedly playing a role in improving existing solar cell systems, such as dye sensitized solar cells (DSSCs) and perovskite solar cells (Zhang and Shi, 2011).

In addition, three-dimensional (3D) interconnected graphene network such as aerogels, hydrogels and foams has also attracted a tremendous research attention in the recent years (Zhang et al., 2018). Different approached have been employed to assemble 2D graphene into their 3D forms, Geletion is one of the reported effective approaches for assembling graphene oxide (GO) sheets into 3D graphene hydrogels and with subsequent freeze-drying process could transform hydrogel into 3D graphene aerogel (Zhang et al., 2018). Several reduction methods have been explored to synthesise 3D porous graphene macrostructures, such as hydrothermal method (Zhang and Shi, 2011), solvothermal approach (Liu et al., 2014), chemical reduction (Sui et al., 2011) and electrochemical reduction (Chen et al., 2012) and (Chen et al., 2012).

Template (hard or sorft) directed methods to prepare 3D graphene have received most attention because it can be used for large-scale 3D graphene frameworks. Hard template directing such CVD method has been widely used to fabricate large-scale 3D graphene frameworks by using 3D nickel foams as templates (Zhang et al., 2018). The mechanism is the same as the CVD fabrication of large-scale graphene films, including the pyrolysis of the carbon source, the dissolving of carbon atoms in Ni, and the formation of graphene on Ni surface during the cooling down process (Zhang et al., 2018) and (Yu et al., 2008). Another hard template directing is ice-templating which is simple and environmentally friendly, without the need for the complicated template etching step using strong solvents and acids (Zhang et al., 2018). Besides the hard template directing method, soft templates, such as micelles, emulsions, and bubbles have explored to prepare graphene-based 3D macroscopic structures. 3D graphene-based materials have found its way into energy conversion fields, such as dye-sensitized solar cells (DSSC). 3D nanofoam of graphene has been employed as an alternative to a platinum counter-electrode for DSSC (Tang et al., 2013) which will be discussed in section 6.

5. Application of graphene based photoanode of DSSC

The graphene and graphene derivatives have mostly functioned as a supporting role in the structure of DSSC's photoanode. This section focuses on the use of graphene materials as transparent conductors, in the semiconducting layer, and as the sensitizer (dye).

5.1. Transparent conductive electrodes

Graphene is ramarkable for its several appealling properties in terms of optical transparency, electric conductivity, mechanical strength, and thermal conductivity. Graphene is a super light material with a planar density of 0.77 mg/m^2; the graphene's one atomic layer of carbon atoms is the reason for its advantages of being super thin and ultralight (Zhen et al., 2018). One of the benefits from one atomic thickness is the high transparency of 97.7% in the visible region (Nair et al., 2008). As suggested by both theoretical and experimental results, optical property of graphene can be manipulated by its thickness (Zhen et al., 2018) and (Ni et al., 2007). Considering the high optical transmittance and electrical conductivity of graphene, thin film electrodes made from graphene has become a very competitive transparent conductive material which have been considered a potential candidate to replace many traditional transparent conductive electrode (TCE) such as indium tin oxide (ITO), and fluorine doped tin oxide (FTO) (Zhen et al., 2018) and (Zheng and Kim, 2015). The use of graphene in this area could solve the problem of fragility, environmental pollution, and limited indium resources. Many recents research works have recorded successes using transparent and conductive graphene electrodes to replace the conventioal transparent conducting oxides (TCOs) in dye-sensitized solar cells (Zhang et al., 2015) and (Wang et al., 2008).

It was reported by Bonaccorso et al., (Bonaccorso et al., 2010) that each layer of graphene absorbs about 2.3% of light thereby resulting to 90% transmittance in which light can pass through a maximum of ~5sheets (Bonaccorso et al., 2010). Meanwhile Punkt *et al.,* (2013) showed that for a single-sheet measurement, the thermally reduced graphene oxide (TRGO) sheet with atomic carbon to oxygen ratio higher 300 have R_{Sh} of ~7.7 kΩ/sq (Fig. 7B) (Punkct et al., 2010), while that for pristine graphene is ~6.45 kΩ/sq, (Novoselov et al., 2004). Joseph and Askay (2014) further suggested that this as a result of the layers of the material only been to achieve R_{Sh} around 1 kΩ/sq and transmittance of 90%, even before accounting for contact resistances between individual sheets (Roy-Mattew and Aksay, 2014).

Studies showed that the fabrication of graphene in DSSCs using it as a transparent electrode was first carried out by Wang et al., (Wang et al., 2008) of which graphene films were produced by exfoliating the graphene oxide and then thermally reducing the platelets, thereby forming the TRGO films: The films were formed by sequential dip coating of graphene oxide onto silica glass and then annealing the films at 1100 °C (Wang et al., 2008). High-temperature processing was required in order to reduce the material sufficiently, increasing the size of sp^2-hybridized aromatic networks and increasing conductivity. Those characterized for use as DSSC window electrodes were about 10 nm thick and had R_{Sh} of 1.8 kΩ/sq and a transmittance or about 62% at 550 nm (see Fig. 8).

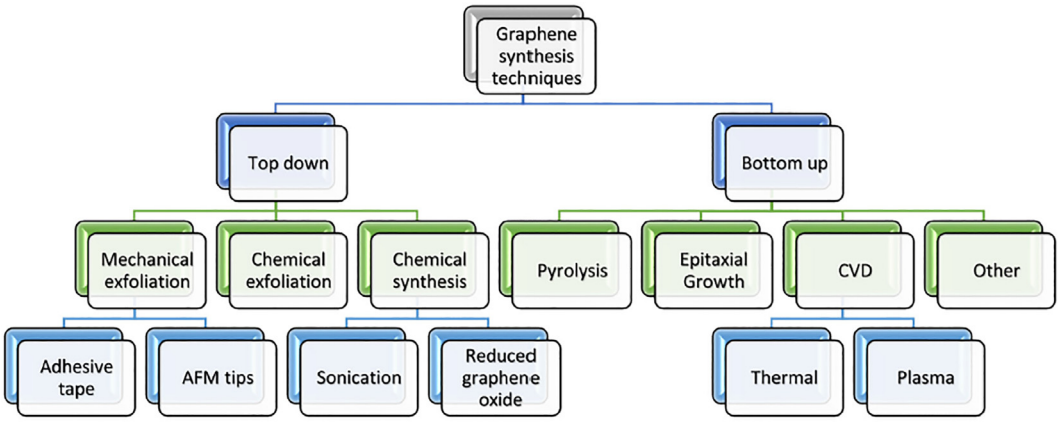

Fig. 7. A process flow chart of Graphene synthesis (Bhuyan et al., 2016).

The films produced as window electrode consists of a wavelength ranging from 1000 nm to 3000 nm and conductivity of 500 Scm^{-1} and a transparency greater than 70% which was however low in performance compared to FTO. However the success recorded by Wang et al., (Wang et al., 2008) became an eye opener to researchers to further advance in the use of graphene as transparent conducting materials (Wang et al., 2008). In a recent research conducted by Zhao et al., (Zhao et al., 2015), it was found that high porosity and large specific surface area was attained by using graphene and titanium film electrodes to promote adsorption rate of sensitizing dye and the PCE was found to be 7.2% (Zhao et al., 2015). In 2013, Lee et al., (Lee et al., 2013) used graphene having monolayer with TiO_2 as photoanode and it resulted to increased PCE by 31% over that of a TiO_2 anode (Lee et al., 2013). Meanwhile in 2012, the values obtained from the results of Huang et al., (Huang et al., 2012) after preparing graphene films on SiO_2 substrates reached a photovoltaic efficiency of over 4.25% and can be compared to FTO used as electrodes (Lee et al., 2014).

In a bid to standardize the comparism of various techniques, De and Coleman (De and Coleman, 2010) analyzed over 20 studies of graphene material-based transparent electrodes. They related the conductivity and transmittance of the material through the ratio of the dc conductivity (σ_{DC}) to the optical conductivity (σ_{Op}) and then related it to the electrode properties (Huang et al., 2012).

Their analysis indicated that the reduced graphene oxide are severely limited by contact resistance between sheets (σ_{DC}/σ_{Op} limit of 0.7), with larger sheets (such as achieved by the Zheng et al. approach or by CVD methods) achieving higher conductivity due to fewer contact regions. They stated that in order to achieve a 100 Ω/sq film at a transmittance of 90%, σ_{DC} /σ_{Op} must be 35 or greater. Through their calculations, CVD-derived graphene is more suitable than a mosaic of sheets (σ_{DC}/σ_{Op} limit of 2.6), but it is still far from meeting commercial needs (Roy-Mattew and Aksay, 2014). However, De and Coleman (2011) noted that, the conductivity limit can be increased greatly by increasing the carrier concentration through substrate interactions or electronic doping (Huang et al., 2012). Electronic doping can occur through incorporation of electron-donating or accepting species into the graphene lattice or more commonly through adsorption of these species on sheets. Both HNO_3 and $SOCl_2$ are common examples of chemicals used for the latter electronic doping method. By electronic doping, Zheng *et al.,* (2011) decreased R_{Sh} in their TRGO films almost 25% to 459 Ω/sq at a transmittance of 90% and these brought about a significant improvement but still over an order of magnitude more resistive than ITO films (De and Coleman, 2010). Researchers have embarked on alternate approaches in other to achieve high performance of which the formation of hybrid materials is one of them (Tang et al., 2013); (Zhang et al., 2011) , {1 3 9} and (Kavan et al., 2011). The use of CVD derived graphene and chemically reduced graphene oxide (CRGO-CNT) hybrid films have been produced, as CRGO-(silver nanoparticle) hybrid films. Joseph and Askay (2014) identified grapheme based TCFs produced with CVD as the best having a good performance through its metal nanowire films (Roy-Mattew and Aksay, 2014). Zhu et al., (Zhu et al., 2011) created metal nano-grids (Au, Cu, and Al) with grid lines 100 nm thick and 5–10 μm wide, spaced 100–200 μm apart. CVD derived graphene was then used to coat the grid and form a continuous conductive network (Kavan et al., 2011). Despite the success recorded so far, the scalability of the technology and cost reductions still remain a major issue which calls for serious research attention.

However, recent researches have shown that the graphene based photoanode of DSSC are made from Graphene Oxide (GO) and Reduced Graphene Oxide (rGO). In order to achieve these in graphene-based

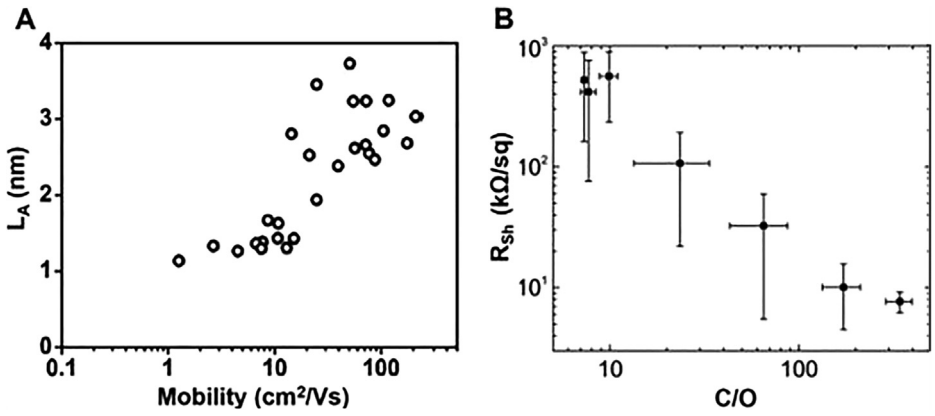

Fig. 8. Relations of structural and electrical properties of RGO (Punkct et al., 2010).

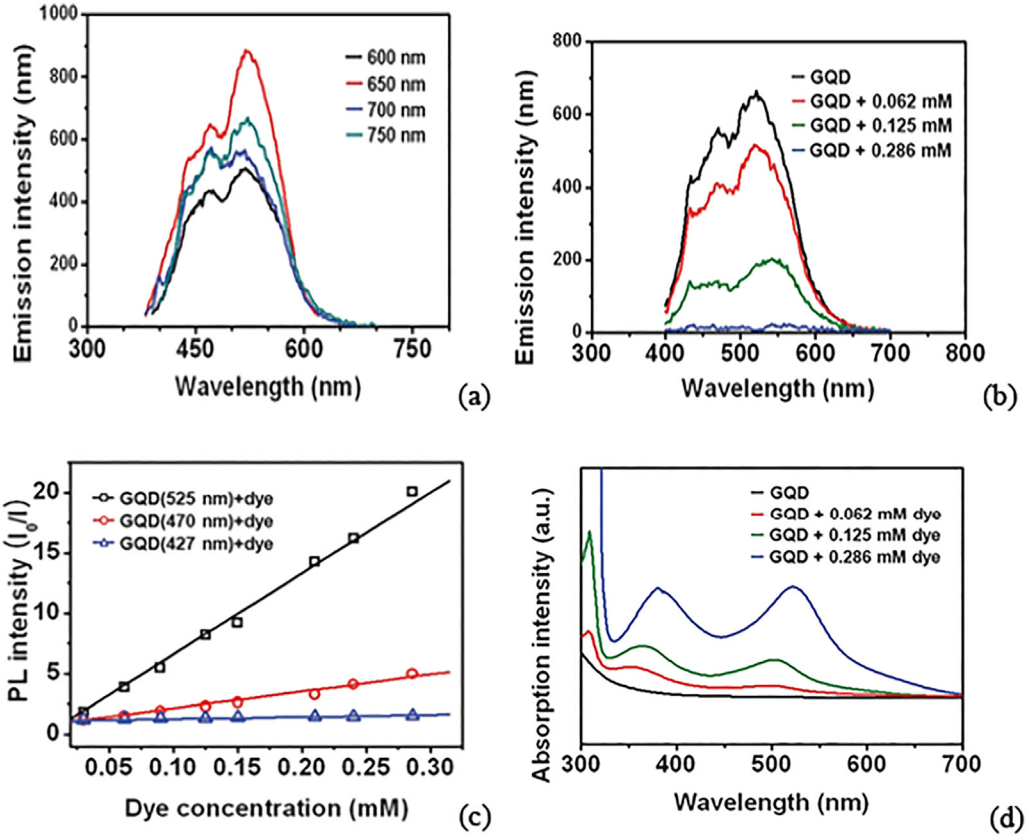

Fig. 9. (a) Upconverted PL spectra of the GQDs at different excitation wavelengths. (b) Fluorescence spectra of GQDs as a function of the amount of dye molecules from 62 to 286 μM. (c) Stern–Volmer plots of the fluorescence quenching of GQDs with the N719 dye. (d) Absorption spectra of GQDs as a function of the amount of dye molecules from 62 to 286 μM (Lee et al., 2013).

electrode, the layer of the thickness can be varied thereby affecting its quality as a result of the GO and rGO. As discussed earlier thermal reduction and the chemical vapor deposition are the two common method of preparation of DSSC meanwhile rGO was prepared with Langmuir–Blodgett method and modified the FTO films in order to cause a reduction in the charge recombination at the interface of TiO_2 and FTO (Zheng and Kim, 2015), although considering a large scale preparation, the CVD approach have gained wider attention. The need for a high-quality preparation of graphene can never be overlooked as more studies are ongoing owing to cracking caused by reduced mechanical strength and poor transfer process resulting from defects. Also, catalytic reactivity often leads to high ratio of wastage of electrons especially when the graphene surface is without proper coverage is exposed to the electrolyte, which is undesirable for a graphene electrode solely serving as a current collector (Seok-Soon et al., 2006)

5.2. Nanostructured semiconductor

In another development, graphene has the potential to form a good contact with nanostructured or mesoporous semiconductors such as nanocrystalline TiO_2 which may benefit the charge separation and conduction. In DSSCs, photo excited electrons are normally injected from the sensitizer to the semiconductor where it will diffuse into the current collector. Numerous reasons can lead to losses of which the fall in voltage occurring in the dye LUMO level and the Fermi level of the semiconductor, from the ohmic resistance in the semiconducting layer, and from recombination of injected electrons with the dye or with oxidized species of the redox couple. More also, the semiconductor or current collector electron (i.e., FTO) can combine again with the electrolyte (Roy-Mattew and Aksay, 2014). Since triiodide tends to combine with FTO, Graphene has been used as the layer that blocks and prevent recombination and also in the TiO_2 scaffolding, this is done so that the photocurrent density can be improved so as to find out the rationales provided (e.g., of light scattering, absorption of dye and the improvement of transported electron) for the observed improved performance (Zhang et al., 2015).

Kim *et al.* were the first to report the use of a graphene material in DSSC as a semiconductor layer which was done photo catalytically by reducing the graphene oxide – TiO_2 nanoparticle composite (TiO_2 particle diameter < 10 nm) as a barrier primarily because the flat sheets could be deposited at temperatures that are low without the use of hazardous chemicals, unlike the common $TiCl_4$ treatment, to provide a blockage in between FTO and triiodide. There was about 7.6% improved performance relatively in the efficiency over a cell without a blocking layer in their result obtained. Meanwhile the result showed that significant absorption of the light from the film had dropped from 85% to 78% in transmittance, which indicated that the approach does not appear better than the normal TiO_2 blocking layers. Though, numerous researches have recorded success in this area using similar approaches and saw improvements (Chen et al., 2012) and (Tang et al., 2013). For instance, Chen et al.(2012) tried using thermally reduced oxides of graphene as a blocking layer which resulted to about 8.1% efficient cell and it was more effective than that without a blocking layer ($\eta = 7.2\%$) and better than one with their $TiCl_4$ pre-treatment blocking layer ($\eta = 7.5\%$) (Chen et al., 2012) and this improved performance was as a result of an increment of the photocurrent. It has been noted that oxides of graphene will cause a blockage for the recombining of electron with the FTO also providing a non-conducting blockage, hence only layers that a very thin that allowed tunneling will be efficient. Therefore, only materials of graphene can will perform optimally as a blocking layer though they should be less active for the redox mediator than FTO (Roy-Mattew and Aksay, 2014).

A more established use of graphene materials has been their incorporation into the semiconducting layer itself purposely to optimize the performance of the device by ensuring that the charge collection efficiency, (i.e., photocurrent, in the photoanode) in increased (Zhang et al., 2015) and (Roy-Mattew and Aksay, 2014). Incorporating graphene into TiO_2 can cause dye to be absorbed better and improvement

Table 1
Comparing DSSC Performance Parameters between Devices Using Graphene Material Containing Hybrids as the Catalyst and Platinum for Control Cells.

Cathode	Electrolyte	J_{sc} (ma/cm^3)	V_{oc} (V)	FF	η (%)	% change from Pt	Ref
	Iodolyte AN-50, CAN solvent	7.9	0.73	0.72	4.16		(Kou et al., 2011)
Vor-ink TRGO-based films		7.8	0.71	0.70	3.83	−8	
Pt	0.6 M DMPIL, 0.1 MLiI, 0.05 M I, 0.3 M	13.1	0.72	0.68	6.30		(Roy-Mayhew et al., 2010)
Nanoparticles 1 wt% pyrenebutyrate-functionalized graphene, PSS/PEDOT	TBP in 80% CAN/20% THF	13.0	0.72	0.48	4.50	−29	
Pt	0.6 M BMII, 0.03 M I2, 0.5 M TBP,	9.4	0.77	0.70	5.03		(Hong et al., 2010)
N-doped CRGO, 10 wt% PVDF, 5 wt% CaB	0.1 M GSCN in 85% ACN/15% VN	10.6	0.82	0.55	4.75	−6	
Pt	0.5 M LiI, 0.05 M I2, 0 5 M TBP in85%	9.1	0.67	0.55	3.37		(Kaniyor and Ramaprabhu, 2011)
TRGO with nation binder	ACN/15% VN	7.7	0.68	0.54	2.82	−16	
Pt	0.3 M MPII, 0.3 M LiI, 0.05 M I2, 0.3 M	14.2	0.70	0.70	6.88		(Roy-Mayhew et al., 2012)
TRGO, polyanaline	TBP in MPN	13.3	0.69	0.67	6.09	−11	
Pt nanoparticles	0.6 M DMPII, 0.1 M LiI, 0.05 M I2, 0.5 M TBP in CAN	16.0	0.72	0.72	8.34		(Lee et al., 2012)
CRGO, polypyrrole	0.6 M DMPII, 0.1 M LiI, 0.05 M I2,	15.8	0.73	0.71	8.14	−2	(Gong et al., 2013)
Pt nanoparticles	0.5 M TBP in ACN	9.4	0.74	0.66	4.5		
TRGO, PDDA		9.1	0.71	0.47	3.10	−31	
TRGO		8.9	0.70	0.40	2.50	−44	
TRGO, PSS		8.7	0.69	0.35	2.10	−53	
Pt	0.6 M MHII, 0.1 M LiI, 0.05 M I2, 0.5 M TBP in MPN	14.6	0.69	0.73	7.29		(Li et al., 2011)s
TRGO (no substrate)		13.9	0.60	0.18	1.50	−79	
	0.6 M MPII, 0 5 M LiI, 0.05 M I2, 0.5 M TBP in ACN	5.1	0.68	0.59	2.00		(Kaniyor and Ramaprabhu, 2012)
TRGO, Ni nanoparticles		5.2	0.70	0.60	2.19	10	
Pt-nanaoparticles	0.6 M DMPII, 0.1 M LiI, 0.05 M I2,	13.1	0.74	0.62	6.08		(Bajpai et al., 2012)
CRGO, Ni12Ps nanoparticles with carboxymethyl cellulose binder	0.5 M TBP in ACN	12.9	0.73	0.61	5.70	−6	
Pt (PLD)	0.6 M MPII, 0.5 M LiI, 0.05 I2, 0.5 MTBP in CAN	5.8	0.69	0.53	2.11		(Kaniyor and Ramaprabhu, 2012)
TRGO, R(PLD)		6.7	0.74	0.59	2.91	38	
Sputtered Pt	0.6 M DMPII, 0.1 M LiI, 0.05 M I2,	15.3	0.71	0.75	8.16		(Dou et al., 2012)
T-CRGO, Pt nanoparticles (layer by layer EPD)	0.5 M TBP in ACN	15.2	0.71	0.71	7.66	−6	
	E008: 0.1 M I2, 1 M MPII, 0.5 M NMB,	13.1	0.72	0.67	6.29		(Gong et al., 2011)
Coreduced GO, Pt nanoparticles	0.1 M LiTFSI in MPN	14.1	0.72	0.67	6.77	8	
Evaporated Pt	0.6 M BMII, 0.03 M I2, 0.5 M TBP,	10.6	0.73	0.68	5.27		(Tjoa et al., 2012)
Coreduced GO, Pt nanoparticles	0.1 M GSCN in 85% ACN/15% VN	12.1	0.79	0.67	6.35	20	
Sputtered Pt	1 M DMII, 0.15 M I2, 0.5 M TBP, 0.1 M	13.4	0.72	0.66	6.38		(Yen et al., 2011)
TRGO, MoS_2nanoparticles with 10 wt% PVDF, 10 wt % CaB	GSCN in MPN	12.5	0.73	0.66	6.04	−5	

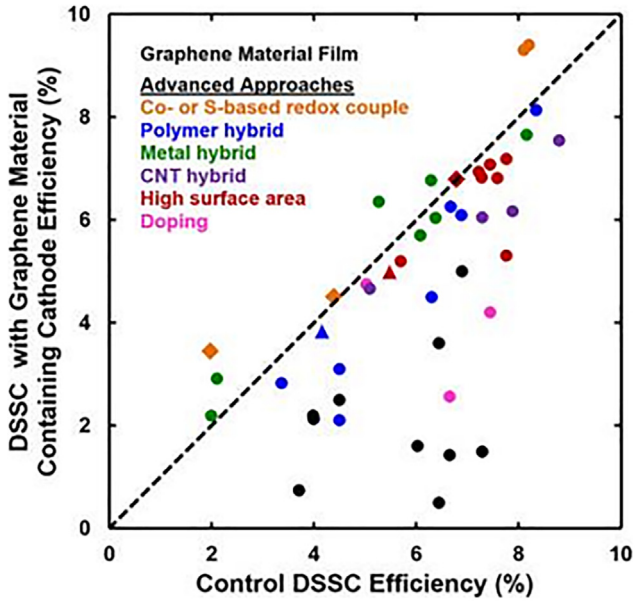

Fig. 10. Comparison of reported efficiencies for DSSCs with and without graphene materials as the cathode catalyst (Roy-Mattew and Aksay, 2014).

in the separation of charges, alongside with an accelerated photogenerated electron transport hence minimizing the rate at which charges recombine (Zhu et al., 2011) and (Low and Lai, 2018). Yang et al., (Yang et al., 2010) discovered that graphene could combine with TiO_2 nanoparticles to produce bridges of graphene thereby enhancing the rate at which charges are transported and this will not allow the recombination of charges and light collection increase of the device (Yang et al., 2010). Normally, DSSCs have about 10–20 μm layer of TiO_2 that is thick. Therefore, electrons that are photogenerated in the back side have to spread out to the front to be received, a length of which the order is about 100 μm assuming a random walk. The efficiency at which it is received is a function of electron diffusion length and the thickness of the film can be approximated by observing the transported electron and the time scale at which the electrons recombine (Roy-Mattew and Aksay, 2014). A way to ensure that the efficiency of collection efficiency increases is to make sure that the transported electrons in the TiO_2 (i.e., increase the length at which the diffusion occur) is improved and this should occur with the sintering process. Another way to this is to reduce the distance of the electron path, and this can happen when finger electrodes is created into the layer of TiO_2 (Chen et al., 2013) and (Joanni et al., 2007). These approaches suffered a significant drawback by the primary particle size of ITO or tin oxide used in the electrode materials as well as by the need to coat the conducting fingers with a blocking layer of TiO_2 (at least 6 nm) to prevent recombination in the device (Zhu et al., 2011). Overcoming this, materials of graphene materials has a specific advantage because of their atomic thinness and high aspect ratio that provides a very low

percolation threshold and can serve as a collector of current with a little variation of the TiO_2 film morphology (Roy-Mattew and Aksay, 2014).

Sun et al., (Sun et al., 2018) explained that such hybrid nanostructures establish physical adsorption (physisorption), electrostatic binding, and charge transfer interaction between graphene and TiO_2 nanoparticles leading to a reduction of TiO_2-TiO_2 contact resistance (Chappel et al., 2005). Owing to graphene's perfect conduction of electricity, the bridged graphene acts as a channel in which electrons can be transferred to improve the transportation of electrons from the conduction band (CB) of TiO_2 at the anchor position quickly, thus reducing recombination. When graphene is introduced, it causes more holes inside the photoanode which would be helpful to enhance the absoption of light and the effciency of collection, thereby, resulting to improved performance of DSSCs (Chappel et al., 2005) and (Sun et al., 2018).

Several studies have incorporated graphene materials into semiconductor films in a various ways, some of the research claimed that when TiO_2 conductivity is increased, there is improvement and that is the main reason for it (Yang et al., 2010). While others believed otherwise and that improvement is caused by increased dye loading and light scattering in the electrode which unforeseen side effects (Zhang et al., 2015). The reports connotes that at the states in wich the photogenerated electrons are excited, they are injected into the CB of TiO_2 and thereby optimizing the PCE of the DSSCs. That is to say that, when the graphene materials is in excess, there would be a reduction of PCE of DSSCs due to the decrement of the absorption of light of the dye as TiO_2 was covered by the graphene. Nevertheless, excessive graphene content will also increase the electron-hole pairs' recombination rather than generate electrons pathway in DSSCs.

5.3. Dye molecule (Sensitizer)

Generally, the sensitizing dye carries out two functions which are light absorption and transfer of electrons to the conduction band of the semiconductor. A sensitizing dye that is efficient should possess absorption that is intense in the visible region thereby possessing high extinction coefficient which has strong adsorption affinity to the surface of the semiconductor, and stability in its oxidized form (Roy-Mattew and Aksay, 2014). More also, it is able to exhibit more negative lowest unoccupied molecular orbital (LUMO) energy than the conduction band (CB) of the semiconductor (usually TiO_2) and more positive highest occupied molecular orbital (HOMO) energy than the redox potential of the electrolyte (Zhang et al., 2015) as shown in Fig. 2. The expensive price of Ru-based dyes for DSSCs has necessitated consideration for cheaper alternative materials. As a result, the use of graphene has been a research focus for this purpose and since the band gap of graphene is tunable, it is considered for dye co-sensitisation in a DSSC structure. In addition to suitable band gap, graphene possesses excellent ability of injecting electrons into TiO_2. Recent studies have shown that graphene materials (usually Graphene Quantum Dots (GQDs)) can act as light absorbers in DSSCs (Long et al., 2012); (Yang, 2017) and (Zheng et al., 2012) (Yum et al., 2011). Yan et al., (Yan et al., 2010) used sixty benzene rings and an absorption band at 900 nm, covering all visible lights to synthesize a graphene quantum dot; this material was used as light absorber in DSSC (Zheng et al., 2012). It was found that the devices efficiency was poor, this was attributed to poor contact between graphene and TiO_2. Nevertheless, there is a recent promise in hot injection and multiple carrier generation, providing a means to surpass the Shockley – Quiessar efficiency limit inherent to current device structures (Roy-Mattew and Aksay, 2014).

In spite of the reported graphene poor performance in this role, there had been renewed efforts to co-sensitise dyes in a DSSC to improve the device efficiency since it was observed that the use of GQDs only cannot produce the required efficiency. Fang *et al.,* (2014) observed that the power conversion efficiency (PCE) moved from 5.1% to 6.1%, by putting GQDs into the dye molecules. Similarly, (Mihalache et al., 2015) a DSSC with a co-sensitised dye molecules with GQDs was made and the PCE of the device was improved from 1.92% to 2.12% which was ascribed to co-sensitisation effect of GQDs (Yan et al., 2010) and (Fang et al., 2012). Meanwhile the result obtained by Lee et al., (Lee et al., 2013) and Zhu *et al.,* (2015) showed that by using the GQDs as a co-sensitiser simply by oxidizing the herringbone-type carbon nanofibers mixed with a varying ratio of N719 dye molecules showed a photoluminescence behavior of the GQDs. The result from both studies implied that the GQDs has an up-conversion photoluminescence characteristics with emission band of about 525 nm and a wavelength rising from 600 to 750 nm as shown in Fig. 9a (Lee et al., 2013). Thus, the dye performance was improved by the GQDs at different concentration of the dye and light wavelength, which shows that the up-conversion ability transfers a longer wavelength of photon energy to the area of highest efficiency of the dye molecule Fig. 9(b-d)., thereby improving the efficiency from 7.28 to 7.95% as shown in Fig. 9a.

The use of GQDs as a co-sensitizer is still attracting attention as authors are still exploring better ways of combining it with other materials as well as varying the ratio that would improve the efficiency of the cell. The use of polymer, N3 or N719 dyes as well as even varying size of the GQD have shown considerable improved PCE. Although to overcome intrinsic limitations to conventional devices, researchers need to take advantage of these quantum effects of graphene alongside an ultrafast process of injection.

6. Application of graphene based counter electrode in DSSC

In order for the redox mediators in the DSSCs for charge transport to function efficiently, the following conditions must be met; (i) the redox species must be able to readily diffuse between the anode and the cathode, (ii) the rate of dye regeneration from the reduced species must be faster than from the semi conducting scaffold, and (iii) the rate of reduction of the redox species must be slow at the anode and fast at the cathode.

The use of platinum as counter electrodes in DSSCs has gained widespread usage by depositing it on the FTO of the cell as a result of their high activeness and non-complex mode of fabrication, most especially when using the iodide/triiodide as a mediator (Mihalache et al., 2015). However, there has been some controversies in regards to platinum been stable when used in DSSCs as a result on the decrease in performance of over 11 000 h testing period (Murakami and Gratzel, 2008). Meanwhile as a result of the cost implication involved in the fabrication of Platinum in low cost DSSCs at high temperatures (Roy-Mattew and Aksay, 2014), alternative means have been sought to use carbon black and graphite as its counter electrode. The use of materials made from graphene was introduced in 2008 and this have given rise to countless numbers of research depicting the efficiency diverse graphene materials as a substitute for effective performance and counter electrode optimization of a DSSCs (Desilvestro et al., 2010). Table 1 is shown below to compare platinum based counter electrode and their respective graphene material.

Countless numbers of research have been published ever since 2008 in other to analyze how the catalytic performance is affected by the degree of reduction. (Chen et al., 2012); (Hong et al., 2008) ; (Choi et al., 2011) and (Hsieh et al., 2012) these studies found out that the activity decreased when temperature of thermal annealing activity of porous CRGO films was raised to 400 °C in air. The result obtained from the RCT for the T-CRGO film at 400 °C when compared to that heated to about 250 °C showed that the latter was about 280 times higher while Choi et al., (Choi et al., 2011) reported the lowest and was similar to the treatment reported above (Hong et al., 2008). Another research carried out by Choi et al., (Choi et al., 2011) depicted that there was a decrease monotonically in RCT for CRGO which were thermally treated at very high temperatures of about 600 °C progressively, of which was the highest used during their research (Hong et al., 2008). Meanwhile another study conducted by Hsieh et al., (Hsieh et al., 2012) showed also a

similar increase in the performance but this was obtained from reducing the temperature of the oxides of graphene, with films (20 μm thick with 5% polyvinylidene fluorine, PVDF) annealed at 700 °C exhibiting an RCT of 22Ωcm^2 (Choi et al., 2011).

Relatively inert materials have limitations and in order to overcome it, improving morphology, generally by ensuring that the size of the pores and the area of its was increased, chemically modifying the intrinsic activity of the material which will in turn increase it must be carried out (Roy-Mattew and Aksay, 2014). In other to improve the morphology, material used must be increased and the film to be used must be thickened. In a study earlier carried out by Wu and Zheng (2013) using electrophoretic deposition and spin coating methods, a vertically oriented CRGO and a horizontally oriented CRGO respectively was created by them (Jang et al., 2012). The work depicted that the activity of the vertically oriented CRGO was greater, proposing that the mobility of the ion and accessible area of its surface was high in the system. Meanwhile, the procedure for deposition uses $NiCl_2$, therefore the fact that the improved performance resulting from the 1 wt% of Ni which was deposited in the course of the reaction can't be overlooked (Roy-Mattew and Aksay, 2014). An earlier research conducted by Zheng et al., (Zheng et al., 2012) indicated that when CRGO in poly (ethylene glycol) is grinded and the polymer which lead to the films of which its pore spaces are larger (by ~1 nm) is thermalized and DSSCs with higher efficiencies (η = 7.2%) than those created from ultra-sonicating CRGO in the polymer (η = 5.2%) (Yang, 2017).Even so, these devices still did not match the performance of those using platinized FTO (η = 7.8%) (Roy-Mattew and Aksay, 2014). In other to increase the area of the surface of the electrodes, Lee et al., (Lee et al., 2012) was the first to create a $NiCl_2$ − poly (vinyl alcohol) film after which pyrolysis was done on it to produce a substrate of nickel which is porous. This was possible with the use of CVD and the etching of the metal scaffold was done subsequently to give a pore diameter of about 40–50 nm which are porous hence graphene structures that are derived from CVD method. Gong et al., (Gong et al., 2012) undertook a different method which was to separate the RGO sheets thereby making them apart thus increasing the area of the surface. The spacers that was used in increasing the CRGO film from a specified area of 8.6 to 383.4 m^2/g was a 12 nm size particle of SiO_2 (Shixin et al., 2013). Despite the success attained so far, platinized FTO had a better performance of about 6% compared to the thin film that was produced with spacers. On the other hand the performance of the FTO that was platinized was matched in 2012 by Roy *et al.,* (2012) with an efficiency of 6.8% for both. This was done by using ethyl cellulose binder to doctor blade a TRGO film and the binder was partially thermalized, thereby disrupting the restacking of the TRGO films as a result of the insoluble residue that was left behind (Gong et al., 2012).

The process of hybridizing graphene materials and polymers is another way of improving its characteristics of which it has been extensively researched on. These characteristics comprises of adhesion, durability, conductivity, and catalytic activity. A typical application is the use of Nafion and polyvinylpyrrolidone binders in TRGO films, however some catalytic limitations were encountered resulting to its porosity been very low. Another one was done with the use of HNO_3-doped CVD derived graphene which has four layers were used as a conductive substrate for about110 nm poly(3,4-ethylenedioxythiophene) (PEDOT) films (Roy-Mattew and Aksay, 2014). RGO has also been used as a scaffold for polymer nucleation for polyanaline and for polypyrrole (Shixin et al., 2013) and (Roy-Mayhew et al., 2012).

Only a few studies have succeeded in matching the performance of platinum as a catalyst using graphene materials amongst many others as shown in Fig. 10. The formation of TRGO at a very high temperature performs better than pristine graphene or CRGO; although, the availability of iodide/triiodide redox couple has resulted to large area networks of graphene materials been required (Roy-Mattew and Aksay, 2014). Moreover, this role can still make use of thick layered materials, while the electrodes can become limited as a result of diffusion through a network that is porous which will result to films that are opaque. Different kind of graphene can be suitable when sulfur and cobalt based mediators are utilized however, the TRGO material will require few materials and the presence of defect site and edges enables catalyst to be introduced into it. As a result of the nanoparticles at the defect sites and edges, the TRGO becomes the most promising (Wang, 2012).

7. Conclusion and outlook

Solar energy has gained much relevance today because of the quest for sustainable form of energy and the use of photovoltaic has resulted to its wide application due to its ability to convert the energy from the sun directly to electricity. The DSSC which is the most recent advanced technology of solar cells can only be efficient when its various structures are optimized. The various fabrication techniques of FTO in DSSCs has shown improved optimization, however the incorporation of graphene into the photoanode of DSSCs will enhance its efficiency due to its unique properties. In order to achieve high efficiency, the method of synthesizing graphene into the cell will go a long way to determine the output performance of the cell. Most studies have used the CVD method amongst many others to incorporate graphene into the photoanode were hydrocarbons such as methane is decomposed into graphene using metal surfaces as catalyst. Graphene incorporated DSSCs will lead to better dye absorption, improved charged separation, excellent electrical conductivity thereby resulting in improved performance of the cell. However, further researches are being carried out to find out the effectiveness of FTO in DSSCs incorporating graphene material to the photoanode as well the counter electrode.

Acknowledgement

The authors of this research specially appreciate the University of Witswatersrand (Wits), Johannesburg, South Africa and the Petroleum Training Institute, Effurun, Delta State, Nigeria for their immense support offered.

References

Ahmad, D., Choi, W.J., Seo, Y.I., Seo, Sehun, Lee, Sanghan, Park, Tuson, Mosqueira, J., Genda, Gu., Kwon, Yong Seung, 2017a. Effect of proton irradiation on the fluctuation induced magnetoconductivity of FeSe1 − x Tex thin films. New J. Phys. 19.

Ahmad, M.S., Pandey, A.K., Abd'Rhahim, N., 2017b. Advancements in the development of TiO_2 photoanodes and its fabrication methods for dye sensitized solar cell (DSSC) applications. A review. Renew. Energy Rev. 77, 89–108.

Anwar, Hafeez, 2013. Precious Metal-free Dye-sensitized Solar Cells. Dalhousie University, Halifax, Nova Scotia.

Aoki, H., Dresselhaus, M.S., 2014. Preface. In: Aoki, H., Dresselhaus, M.S. (Eds.), Physics of Graphene. Springer, Cham, Switzerland, pp. v–vi.

Aouaj, M.A., Diaz, R., Belayachi, A., Rueda, F., Abd-Lefdil, M., 2009. Comparative Study of ITO and FTO Thin Films Grown by Spray Pyrolysis. Mater. Res. Bull 44 (7), 1458–1461.

Archer, M.D., Nozik, A.J., 2008. Nanostructured and Photoelectrochemical Systems for Solar Photon Conversion. Imperial College Press, London, Vol, pp. 3.

Arons, A.B., Peppard, M.B., 1965. Einstein's Proposal on Photon Concept- A Translation o Annalen der Physik Paper of 1905. Am. J. Phys. 33, pp132.

Bagher, A.M., Mirzaei, M.A., Mohsen, M., 2015. Types of Solar Cells and Application. American Journal of Optics and Photonics 3 (5), 94–113.

Bajpai, Roy, S., Kumar, P., et al., 2012. Graphene supported platinum nanoparticle counter electrode for enhanced performance of DSSC. ACS Applied materials & interface 3 (10), 3884–3889.

Banyamin, Ziad Y., Kelly, Peter J., West, Glen, Boardman, Jeffery, 2014. Electrical and Optical Properties of Fluorine Doped Tin Oxide Thin Films Prepared by Magnetron Sputtering. Coatings 4, 732–746.

Batmunkh, M., Dadkhah, M., Shearer, C.J., Biggs, M.J., Shapter, J.G., 2016. Incorporation of graphene into SnO2 photoanodes for dye-sensitized solar cells. Appl. Surf. Sci. 387, 690–697.

Bhagwat, S., Dani, R., Goswami, P., Kerawalla, M.A.K., 2017. Recent advances in optimization of photoanodes and counter electrodes of dye-sensitized solar cells. Curr. Sci. 113 (2), 228–235.

Bhuyan, Sajibul Alam, Uddin, Nizam, Islam, Maksudul, Alam, Ferdaushi, Hossain, Sayed, 2016. Graphene a two dimensional material for sp2 hybridization of…Nano. letters 6 (2), 65–83.

Bisquert, J., Cahen, D., Hodes, G., Rühle, S., Zaban, A., 2004. Physical Chemical Principles of Photovoltaic Conversion with Nanoparticulate, Mesoporous Dye-

Sensitized SolarCells. J. Phys. Chem. B 108 (24), 8106–8118.
Bisquert, J., Vikhrenko, V.S., 2004. Interpretation of the Time Constants Measured by Kinetic Techniques in Nanostructured Semiconductor Electrodes and Dye-Sensitized Solar Cells. J. Phys. Chem. B 108 (7), 2313–2322.
Boehm, H.P., Clauss, A., Fischer, G.O., Hofmann, U., 1962. The adsorption behavior of very thin carbon films. Journal of Inorganic and General Chemistry B 17, 150–153.
Bonaccorso F., Sun Z., Hasan T., and Ferrari A.C. (2010) Nature photonics.
Bonaccorso, Francesco, Lombardo, Antonio, Hasan, Tawfique, Sun, Zhipei, Colombo, Luigi, Ferrari, Andrea C., 2012. Production and processing of graphene and 2d crystals. Mater. Today 15 (12), 564–589. https://doi.org/10.1016/S1369-7021(13)70014-2.
Boschloo, G., Hagfeldt, A., 2009. Characteristics of the Iodide/Triiodide Redox Mediatorin Dye-Sensitized Solar Cells. Acc. Chem. Res 42, 1819–1826.
Brian O'regan and Michael Gratze. (1991). A low-cost, high-efficiency solar cell based on dye-sensitized colloidal tio 2 films.
Britnell, L., Ribeiro, R.M., Eckmann, A., Jalil, R., Belle, B.D., Mishchenko, A., Novoselov, K.S., 2013. Strong Light-Matter Interactions in Heterostructures of Atomically Thin Films. Science 340 (6138), 1311–1314.
Cahen, D., Hodes, G., Gratzel, M., GuillemolesJ, F., Riess, I., 2000. Nature of photovoltaic action in dye-sensitized solar cells. J. Phys. Chem. B 104 (9), 2053–2059.
Chae, S., Jang, S., Choi, W.J., Kim, Y.S., Chang, H., Lee, T.I., Lee, J.-O., 2017. Lattice Transparency of Graphene. Nano Lett. 17 (3), 1711–1718.
Chappel, S.; Grinis, L.; Ofir, A.; Zaban, (2005). A. J. Phys. Chem. B, 109, 1643. (151).
Chen, Y., Chen, K., Bai, H., Li, L., 2013. Electrochemically reduced graphene porous material as light absorber for light-driven thermoelectric generator. J. Mater. Chem. 22 (34), 17800–17804.
Chen, Y.S.; Lee, J.; Tsai, S.; Ting, C. (2007). Manufacture of Dye-Sensitized Solar Cells and their I-V Curve Measurements. Proceedings of ICAM 2007, Taipei, Taiwan, November 26-28.
Chen, T., Qiu, L.B., Cai, Z.B., Gong, F., Yang, Z.B., Wang, Z.S., Peng, H.S., 2012. Intertwined aligned carbon nanotube fiber based dyesensitizedsolar cells. Nano Lett. 12 (5), 2568–2572.
Choi, J.H., Kang, S.H., Oh, H.S., Yu, T.H., Sohn, I.S., 2011. Design and Characterization of Ga-Doped Indium Tin Oxide Films for Pixel Electrode in Liquid Crystal Display. Thin Solid Films 527, 141–146.
ChunHung, Law, Pathirana, Shehan C, Li, Xaioe, Anderson, Assaf Y, Barnes, Piers RF, Listorti, Andrea, Ghaddar, Tarek H, et al., 2010. Water-based electrolytes for dye-sensitized solar cells. Adv. Mater. 22 (40), 4505–4509.
Cox, S.F.J., Davis, E.A., Cottrell, S.P., King, P.J.C., Lord, J.S., Gil, J.M., Alberto, H.V., Vilao, R.C., Duarte, J.P., De Campos, N.A., Weidinge, A., Lichti, L., Irvine, S.J.C., 2001. Experimental confirmation of the predicted shallow donor hydrogen state in zinc oxide. Phys. Rev. Lett 86, 2601–2604.
De, S., Coleman, J.N., 2010. ACS Nano 4, 2713.
de Moure-Flores, F., Guillen-Cervantes, A., Nieto-Zepeda, K.E., QuinonesGalvan, J.G., Hernandez-Hernandez, A., De La, M., Olvera, L., Melendez-Lira, M., 2013. SnO2: F thin films deposited by RF magnetron sputtering: effect of the SnF2 amount in the target on the physical properties. Rev. Mex. Fis 59, 335–338.
Desilvestro, H.; Boz, M.; Tulloch, S.; Tulloch, G (2010).In Dye Sensitized Solar Cells; Kalyanasundaram, K., Ed.; EPFL Press: Lausanne (189).
Dou, Y.Y., Li, G.R., Song, J., Gao, Y.P., 2012. Nickel phosphate embedded graphene as counter electrode for dye sensitized solar cells. PCCP 14 (4), 1339–1342.
Du, J., Lai, X., Yang, N., Zhai, J., Kisailus, D., Su, F., Jiang, L., 2010. Hierarchically Ordered Macro − Mesoporous TiO2 − Graphene Composite Films: Improved Mass Transfer, Reduced Charge Recombination, and Their Enhanced Photocatalytic Activities. ACS Nano 5, 590–596.
Du, X., Skachko, I., Barker, A., Andrei, E.Y., 2008. Approaching ballistic transport in suspended graphene. Nat. Nanotechnol. 3, 491–495.
Eran, Barnoy, Mark Conley, A., Gan, Stephen, Gefen, Yoni, Lovell, Jana, Mann, Katherine, Shuchatowitz, Adin, Tobin, Christine, 2011. The Potential of Natural. University of Maryland, Photosythentic Pigment to Improve the Efficiency of Dye-Sensitized Solar Cell.
Fang, X., Li, M., Guo, K., Zhu, Y., Hu, Z., Liu, X., Chen, B., Zhao, X., 2012. Improved properties of dye-sensitized solar cells by incorporation of graphene into the photo-electrodes. Electrochim. Acta 65, 174–178.
Fisher, A.C., Peter, L.M., Ponomarev, E.A., Walker, A.B., Wijayantha, K.G.U., 2000. Intensity Dependence of the Back Reaction and Transport of Electrons in Dye-Sensitized Nanocrystalline TiO2 Solar Cells. J. Phys. Chem. B 104 (5), 949–958.
Frank, A.J., Kopidakis, N., van de Lagemaat, J., 2004. Electrons in nanostructured TiO2 solar cells: transport, recombination and photovoltaic properties. Coordination Chem. Rev. 248, 1165–1179.
Ginley, D., Hosono, H., Paine, D.C., 2010. Handbook of Transparent Conductors. Springer Science and Business Media.
Gong, F., Wang, H., Wang, Z.S., 2011. Self assembled mono layer of graphene/Pt as counter electrode for efficient dye sensitized solar cells. PCCP 13 (39), 17676–17682.
Gong, F., Li, Z., Wang, H., Wang, Z.-S., 2012. J. Mater. Chem. 22, 17321.
Gong, F., Xu, X., Zhou, G., 2013. Graphene as counter electrode for DSSC. Electrochim Acta 66, 151.
Granqvist, C.G., 2007. Transparent Conductors as Solar Energy Materials: A Panoramic Review. Sol. Energy Mater. Sol. Cells 91 (17), 529–1598.
Gratzel, M.A., 2003. Dye-sensitized solar cells. J. Photochem. Photobiol., C 4 (2003), 145–153.
Gratzel M., Klug D. R., Durrant J. R. (2008). Dye-Sensitized Mesoscopic Solar Cells. (M. D. Nozik, Ed.) Nanostructured and Photoelectrochemical Systems For Solar Photon Conversion, 3, 503-536.
Green, M.A., 2001. Third Generation Photovoltaics: Ultra-High Conversion Efficiency at Low Cost. Progress in Photovoltaics 9, 123.
Haque, S.A., Tachibana, Y., Willis, R.L., Moser, J.E., Gratzel, M., Klug, D.R., Durrant, J.R., 2000. Parameters influencing charge recombination kinetics in dye-sensitized nanocrystalline titanium dioxide films. J. Phys. Chem. B 104 (3), 538–547.
Hara, K., Horiguchi, T., Kinoshita, T., Sayama, K., Arakawa, H., 2001. Influence of electrolytes on the photovoltaic performance of organic dye-sensitized nanocrystalline tio 2 solar cells. Sol. Energy Mater. Sol. Cells 70 (2), 151–161.
Hong, W., Xu, Y., Lu, G., Li, C., Shi, G., 2008. Electrochem. Commun. 10, 1555.
Hong, Y., Xu, G., Lu, C., Gi, Shi, 2010. Transparent graphene/PEDOT DSSC composite film as counter electrode for DSSC. Electrochemistry 10 (10), 1555–1558.
Hsieh, C.-T., Yang, B.-H., Chen, Y.-F., 2012. Diamond Relat. Mater 27–28, 68.
Huang, S., Sun, H., Huang, X., Zhang, Q., Li, D., Luo, Y., Meng, Q., 2012. Carbon nanotube counter electrode for high-efficient fibrous dye-sensitized solar cells. Nanoscale Res. Lett. 7 (1), 1–7.
Huilei, Zhao, Liu, Lianjun, Andino, Jean M, Li, Ying, 2012. Photocatalytic co_2 reduction with h_2o on tio_2 nanocrystals: Comparison of anatase, rutile, and brookite polymorphs and exploration of surface chemistry. ACS Catal. 2 (8), 1817–1828.
Hussein, I. A., Mehmood, U., and Al-Ahmed, S., (2016). "Enhancing Power Conversion Efficiency of Dye-Sensitized Solar Cell Using TiO2-MWCNT Composite Photoanodes".
International Energy Agency, 2012. Key World Energy Statistics 2012. International Energy Agency, Paris, France.
Jager T., Bissig B., Dobeli M., Tiwari A.N., Romanyuk Y.E. (2014). Thin films of SnO2:F by reactive magnetron sputtering with rapid thermal post-annealing. Thin Solid Films, 553, 21-25.
Jang, H.-S., Yun, J.-M., Kim, D.-Y., Park, D.-W., Na, S.-I., Kim, S.-S., 2012. Electrochim. Acta 2012 (81), 301.
Jang, H.-S., Yun, J.-M., Kim, D.-Y., Park, D.-W., Na, S.-I., Kim, S.-S., 2015. Electrochim. Acta 2012 (81), 301.
Janotti, A., Van de Walle, C.G., 2007. Hydrogen multicentre bonds. Nat. Mater 6, 44–47.
Jayawardena, K.D.G.I., Rozanski, L.J., Mills, C.A., Beliatis, M.J., Nismy, N.A., Silva, S.R.P., 2013. 'Inorganics-in-Organics': Recent developments and outlook for 4G polymer solar cells. Nanoscale 5, 8411–8427.
Joanni, E., Savu, R., de Sousa Goes, M., Bueno, P.R., De Freitas, J.N., Nogueira, A.F., Longo, E., Varela, J.A., 2007. Scr. Mater 57, 277.
John, Anand S., Dancer, Ibrahim, Reddy, Bale V., 2009. Development of New Solar Exergy Maps. Int. J. Energy Res. 33, 709–718.
Jubault, M., Pulpytel, J., Cachet, H., Boufendi, L., Arefi-Khonsari, F., 2007. Deposition of SnO2: F Thin Films on Polycarbonate Substrates by PECVD for Antifouling Properties. Plasma Processes Polym. 4 (S1), S330–S335.
Alan B. Kaiser, Cristina Gomez-Navarro, Ravi S. Sundaram, Marko Burghard and Kluas Kern. (2007). Electrically conduction mechanism in chemically derived monolayers .Nano letters. 9 (5) 1787-1792.
Kang, S.H., Kang, M., Choi, S., Kim, J., Kim, H., 2008. Improved Charge Transport in Dye-Sensitized Solar Cells Employing Viscous Non-Volatile Electrolytes. Electrochem Commun 10, 1326–1329.
Kaniyor, A., Ramaprabhu, S., 2011. Thermally exfoliated graphene based counter electrode for low cost DSSC. J. Appl. Phys. 109 (12), 124308.
Kaniyor, A., Ramaprabhu, S., 2012. Graphene as counter electrode for low cost DSSC. Mater. Chem 22, 8377.
Kavan, J.H., Yum, Gratzel, M., 2011. Optically transmitted cathode for dye-sensitzed solar cells based on grapheme nano platelete. ACS Nano 15 (10), 165–172.
Kay, A., Gratzel, M., 1996. Low cost photovoltaic modules based on dye sensitized nanocrystalline titanium dioxide and carbon powder. Sol Energ Mat Sol C 44 (1), 99–117.
Khamwannah, J. (2015). Design and Fabrication of Efficient Electrodes for Dye Sensitized Solar Cells. UC San Diego: Electronic Theses and Dissertations.
Kim, Seok-Soon, Nah, Yoon-Chae, Noh, Yong-Young, Jo, Jang, Kim, Dong-Yu, 2006. Electrodeposited pt for cost-efficient and flexible dye-sensitized solar cells. Electrochim. Acta 51 (18), 3814–3819.
Kou, R., Shao, Y., Mei, D., Nie, Z., Wang, D., Wang, C., Viswanathan, V.V., Park, S., Aksay, I.A., Lin, Y., 2011. J. Am. Chem. Soc 133, 2541.
Kuciauskas, D., Freund, M.S., Gray, H.B., Winkler, J.R., Lewis, N.S., 2000. Electron Transfer Dynamics in Nanocrystalline Titanium Dioxide Solar Cells Sensitized with Ruthenium or Osmium Polypyridyl Complexes. J. Phys. Chem. B 105 (2), 392–403.
Lavrov, E.V., Borrnet, F., Weber, A., 2005. Photoconductivity and infrared absorption study of hydrogen-related shallow donors in ZnO. Phys. Rev. B 72, 085212.
Lee, J.S., Ahn, H.J., Yoon, J.C., Jang, J.H., 2012. Three dimensional nano foam of few layer graphene grown by CVD for DSSC. PCCP 14 (22), 7939–7943.
Lee, E., Ryu, J., Jang, J., 2013. Fabrication of graphene quantum dots via size-selective precipitation and their application in upconversion-based DSSCs. Chem. Commun. (Camb) 49, 9995–9997.
Lee, K.M., Shih, K.L., Chiang, C.H., Suryanarayanan, V., 2014. Fabrication of High Transmittance and Low Sheet Resistance Dual Ion Doped Tin Oxide Films and Their Application in Dye-Sensitized Solar Cells. Thin Solid Films 570, 7–15.
Lenzmann, F.O.; Kroon, J.M. (2007). Recent Advances in Dye-Sensitized Solar Cells. Advances in OptoElectronics. 1-10.
Li, D., Kaner, R.B., 2008. Graphene-based composite materials. Science 320 (5880), 1170–1171. https://doi.org/10.1126/science.1158180.
Li, S., Qiu, L., Shi, C., Chen, X., Yan, F., 2014. Water-Resistant, Solid-State, Dye-Sensitized SolarCells Based on Hydrophobic Organic Ionic Plastic Crystal Electrolytes. Adv. Mater. 26, 1266–1271.
Li, J., Ye, S., Li, T., Li, X., Yang, X., Ding, S., 2015. Preparation of graphene nanoribbons (GNRs) as an electroniccomponent with the multi-walled carbon nanotubes (MWCNTs). Procedia Eng. 10, 492–498.
Li, X., Zhao, T., Wang, K., Yang, Y., Wei, J., Kang, F., Zhu, H., 2011. Directly Drawing Self-Assembled, Porous, and Monolithic Graphene Fiber from Chemica l Vapor Deposition Grown Graphene Film and Its Electrochemical Properties. Langmuir 27 (19),

12164–12171. https://doi.org/10.1021/la202380g.
Li, X., Zhang, X., Hua, J., Tian, H., 2017. Molecular engineering of organic sensitizers with o, p-dialkoxyphenyl-based bulky donors for highly efficient dye-sensitized solar cells. Mol. Syst. Des. Eng. 2 (2), 98–122.
Liao, B.H., Kuo, C.C., Chen, P.J., Lee, C.C., 2011. Fluorine-doped tin oxide films grown by pulsed direct current magnetron sputtering with an Sn target. Appl. Opt 50, 106–110.
Liao, B.H., Chan, S.H., Lee, C.C., Kuo, C.C., Chen, S.H., Chiang, D., 2014. FTO films deposited in transition and oxide modes by magnetron sputtering using tin metal target. Appl. Opt 53, 148–153.
Bin Liu and Eray S Aydil. (2009). Growth of oriented single-crystalline rutile tio2 nanorods on transparent conducting substrates for dye-sensitized solar cells. Journal of the American Chemical Society, 131(11):3985–3990. (Chowdhurry et al., 2015).
Liu, X., Cui, J., Sun, J., Zhang, X., 2014. 3D graphene aerogel-supported SnO2 nanoparticles for efficient detectionof NO2. RCS Advances 4 (43), 22601–22605.
Liyanage, D., 2013. Ethylene Glycol Assisted Synthesis of Fluorine Doped Tin Oxide Nanorods Using Improved Spray Pyrolysis Deposition Method. Appl. Phys Express 6 (8), 085501.
Long, R., English, N.J., Prezhdo, O.V., 2012. J. Am. Chem. Soc 134, 14238.
Longo, C., Paoli, De, 2003. M-A. Dye-Sensitized Solar Cells: a Successful Combination of Materials. J. Braz. Chem. Soc. 14, 889–901.
Low, F.W., Lai, C.W., 2018. Renewable and Sustainable Energy Reviews. Recent developments of graphene-TiO2 composite nanomaterials as efficientphotoelectrodes in dye-sensitized solar cells. A review 82 (1), 103–125.
Luo, Y., Yuan, B., Yu, Q., Feng, Y., 2012. Substrateless graphene fiber: a sorbent for solid-phase microextraction. J. Chromatogr. A 1268, 9–15.
Mahmoud A.M, Al-Alwani, Abu Bakar Mohamad, Norasikin A. Ludin, Abd. Amir H. Kadhum, Kamaruzzaman Sopian (2016). Dye-Sensitised Solar Cells: Development, Structure, Operation Principles, electron kinetics, Characterisation, synthesis materials and natural photosensitisers, Renewable and Sustainable Energy Review, 183-213.
Maruyama, T., Akagi, H., 1996. Fluorine-doped tin dioxide thin films prepared by radio-frequency magnetron sputtering. J. Electrochem. Soc 143, 283–287.
Mcmaster, H.A., 1947. U. S. Patent No 2 (429), 420.
Gratzel Michael (2005). Photovoltaic performance and long-term stability of dye-sensitized meosocopic solar cells, Published by Elsevier, C.R. Chimie 9 (2006), pp578-583.
Mihalache, I., Radoi, A., Mihalia, M., Munteanu, C., Marin, A., Danila, M., 2015. Charge and energy transfer interplay in hybrid sensitized solar cells mediated by grapheme quantum dots. Electrochim 153, 306–315.
Miles, D., 2015. Anodized ZnO Nanostructures for Next-Generation Photovoltaics. University of Bath, University of Bath.
J. M. Mochel (1947). U. S. Patent No 2,564,706.
Mohammad Bagher, Askari, 2015. Types of Solar Cells and Application. AJOP 3 (5), 94. https://doi.org/10.11648/j.ajop.20150305.17.
Moholkar, A.V., Pawar, S.M., Rajpure, K.Y., Bhosale, C.H., 2008. Effect of concentration of SnCl4 on sprayed fluorine doped tin oxide thin films. J. Alloy. Compd. 455 (1), 440–446.
Muhammad, L.M.N., 2017. Fabrication and Characterization of Nano Structrued Fluorine Doped Tin Oxide Thin Film for DSSC by Hydrothermal Method. Universiti Tun Hussein Onn, Malaysia.
Murakami, T.N., Gratzel, M., 2008. Inorg. Chim. Acta 361, 572.
Murakami, K., Nakajima, K., Kaneko, S., 2007. Initial growth of SnO2 thin film on the glass substrate deposited by the spray pyrolysis technique. Thin Solid Films 515 (24), 8632–8636.
Nair, R.R., Blake, P., Grigorenko, A.N., Novoselov, K.S., Booth, T.J., Stauber, T., Geim, A.K., 2008. Fine Structure Constant Defines Visual Transparency of Graphene. Science 320 (5881) 1308 1308.
Najafi, N., Rozati, S.M., 2017. Structural and electrical properties of SnO_2: F thin films prepared by CVD method. Acta Physica Polonica Series. 131 (1), 222–225.
Naohiko, Kato, Takeda, Yasuhiko, Higuchi, Kazuo, Takeichi, Akihiro, Sudo, Eiichi, Tanaka, Hiromitsu, Motohiro, Tomoyoshi, Sano, Toshiyuki, Toyoda, Tatsuo, 2009. Degradation analysis of dye-sensitized solar cell mo dule after long term stability test under outdo or working condition. Sol. Energy Mater. Sol. Cells 93 (6), 893–897.
Napi Mohd, M.L., Nayan, N., Ahmad, M.K., Fazlee, F.I.M., Hamed, N.K.A., Khalid, N.S., 2016. Fabrication of Flourine Doped Tin Oxide with Different Volume. Sains Malaysiana 45 (8), 1207–1211.
Nazeeruddin, K., Kay, A., Rodicio, I., Humphry-Baker, R., Muller, E., Liska, P., Vlachopoulos, N., Gratzel, M., 1993. Conversion of light to electricity by cis-x2bis (2, 2'-bipyridyl-4, 4'-dicarboxylate) ruthenium (ii) charge-transfer sensitizers (x= cl-, br-, i-, cn-, and scn-) on nanocrystalline titanium dioxide electrodes. J. Am. Chem. Soc. 115 (14), 6382–6390.
Ni, Z.H., Wang, H.M., Kasim, J., Fan, H.M., Yu, T., Wu, Y.H., Shen, Z.X., 2007. Graphene thickness determination using reflection and contrast spectroscopy. Nano Lett. 7 (9), 2758–2763.
Novoselov, K.S., Geim, A.K., Morozov, S.V., Jiang, D., Zhang, Y., Dubonos, S.V., Firsov, A.A., 2004. Electric field effect inatomically thin carbon films. Science 306 (5696), 666–669.
Nurhafizaha, M.D., Suriani, A.B., Mohamed, A., Mamat, M.H., Maleke, M.F., Ahmadf, M.K., Pandikumar, A., Huang, N.M., 2017. Enhanced photovoltaic performance using reduced graphene oxide assisted by triple-tail surfactant as an efficient and low-cost counter electrode for dye-sensitized solar cells. Journal of Optical Material-Elsevier, 291–298.
Oshima, C., Nagashima, A.J., 1997. Ultra-thin epitaxial films of graphite and hexagonal boron nitride on solid surfaces. J. Phys.: Condens. Matter 9 (1), 1–20.
Papageorgiou, N., Maier, W.F., Gratzel, M., 1997. An iodine/triiodide reduction electrocatalyst for aqueous and organic media. J. Electrochem. Soc. 144 (3), 876–884.
Peter, L.M., Wijayantha, K.G.U., 2000. Electron transport and back reaction in dye sensitized nanocrystalline photovoltaic cells. Electrochim. Acta 45 (28), 4543–4551.
Ponomarenko, T., Abdala, A.A., Schedin, F., Kaltnelson, M.I., Yang, R., Novoselov, K.S., Geim, A.K., 2008. Chaotic Dirac billiard in graphene quantum dots. Science 320, 356–358.
Punkct, C, Pope, M. A, Lui , J, Lin Y, Askay, I.A. (2010). Electroanalysis 2010. 22, 2834.
Rho, W.-Y., Song, D.H., Lee, S.H., Jun, B.-H., 2017. Enhanced Efficiency in Dye-Sensitized Solar Cells by Electron Transport and Light Scattering onFreestanding TiO2 Nanotube Arrays. Nanomaterials 7 (345), 1–11.
Roy-Mayhew, Joseph D., Aksay, Ilham A., 2014. Graphene materials and their use in Dye-Sensitized Solar Cells. Chem. Rev. 114, 6323–6348.
Roy-Mayhew, J.D., Bozym, D.J., Punct, C., Askay, I.A., 2010. Functionalized grapheme as catalytic counter electrode in DSSC. ACS Nano 4 (10), 6203–6211.
Roy-Mayhew, J.D., Boschloo, G., Hagfeldt, A., Aksay, I.A., 2012. ACS Appl. Mater. Interfaces 4, 2794.
Sasha, A., Hanif, Mohd, Lau, Mohamad, W.K., Wan Zaki, F.W.S., Ahmad, M.K., 2015. Preparation of Nanostructured Fluorine Doped Tin Oxide (FTO) by Hydrothermal Method. Applied Mechanics and Materials 773–774, 632–636.
Seok-Soon, Kim, Nah, Yoon-Chae, Noh, Yong-Young, Jo, Jang, Kim, Dong-Yu, 2006. Electrodeposited pt for cost-efficient and flexible dye-sensitized solar cells. Electrochim. Acta 51 (18), 3814–3819.
Shah A., Torres P., Tscharner R., Wyrsch N. and Keppner H. (1999). Science, 692-698.
Shixin, Wu., Zheng, Huiqin, Neo, Chin Yong, Quayang, Jianyong, 2013. Highly efficient iodide/triodide Dye sensitized solar cells with gel-coated reduce grapheme.… Applied materials & interface 5 (14), 66657–66664.
Si, Y., Samulski, E.T., 2008. Synthesis of Water Soluble Graphene. Nano Lett. 8 (6), 1679–1682.
Smith, A., 1995. Relation between solution chemistry and morphology of SnO2 based thin films deposited by a pyrosol process. Thin Solid Films 266 (1), 20–30.
Soedergren, S., Hagfeldt, A., Olsson, J., Lindquist, S.E., 1994. Theoretical Models for the Action Spectrum and the Current-Voltage Characteristics of Microporous Semiconductor Films in Photoelectrochemical Cells. The Journal of Physical Chemistry 98 (21), 5552–5556.
Suhaimi, S., et al., 2015. (2015) Materials for Enhanced Dye-sensitized Solar Cell Performance: Electrochemical Application. Int. J. Electrochem. Sci 10, 2859–2871.
Sui, Z., Zhang, X., Lei, Y., Luo, Y., 2011. Easy and green synthesis of reduced graphite oxide-based hydrogels. Carbon 49 (13), 4314–4321.
Sulaeman, U., Abdullah, A.Z., 2017. The way forward for the modification of dye-sensitized solar cell towards better power conversion efficiency. Renew. Sustain. Energy Rev. 74, 438–452.
Sun, Y., Sun, M., Xie, D., 2018. Graphene Electronic Devices. In: Zhu, H., Xu, Z., Xie, D., Fang, Y. (Eds.), Graphene: Fabrication, Characterizations, Properties and Applications. Academic Press, London, United Kingdom, pp. 103–155.
Tahir, A.A., Ullah, H., Sudhagar, P., Teridi, M.A., Devadoss, A., Sundaram, S., 2016. The Application of Graphene and ItsDerivatives to Energy Conversion, Storage, and Environmental andBiosensing Devices. The Chemical Record 16 (3), 1591–1634.
Tang, B., Hu, G., Gao, H., Shi, Z., 2013. Three-dimensional graphene network assisted high performance dyesensitized solar cells. J. Power Sources 234, 60–68.
Tjoa, V., Chua, J., Pramana, S.S., Wei, J., Mhaisalkar, S.G., Mattew, N., 2012. ACS. Appl. Mater Interfaces 4, 3447.
van de Lagemaat, J., Frank, A.J., 2000. Effect of the Surface-State Distribution on Electron Transport in Dye-Sensitized TiO2 Solar Cells: Nonlinear Electron-Transport Kinetics. J. Phys. Chem. B 104 (18), 4292–4294.
Van de Walle, C.G., 2012. Hydrogen as a cause of doping in ZnO. Phys. Rev. Lett 85, 1012–1015.
Wang, H., 2012. Hydrothermal synthesis of hierarchical SnO2 microspheres for gas sensing and lithium-ion batteries applications: Fluoride-mediated formation of solid and hollow structures. J. Mater. Chem. 22 (5), 2140–2148.
Wang, W.Y., Klots, A., Yang, Y.M., Li, W., Kravchenko, I.I., Briggs, D.P., Bolotin, K.I., Valentine, J., 2015. Enhanced absorption in two-dimensional materials via Fano-resonant photonic crystals. Appl. Phys. Lett. 106, 181104.
Wang, DongLin, Su, Gang, 2015. New strategy to promote conversion efficiency using high-index nanostructures in thin-film solar cells. Sci Rep 4 (1). https://doi.org/10.1038/srep07165.
Wang, X., Zhi, L., Müllen, K., 2008. Transparent, conductive graphene electrodes for dye-sensitized solar cells. Nano Lett. 8, 323–327 10.1021/ nl072838r.
Wei, L., Chen, S., Yang, Y., Dong, Y., Song, W., Fan, R., 2018. Effect of Graphene/TiO2 Composite Layer on thePerformance of Dye-Sensitized Solar Cells. J. Nanosci. Nanotechnol. 18 (2), 976–983. https://doi.org/10.1166/jnn.201 8.14186.
Xiang, C., Young, C.C., Wang, X., Yan, Z., Hwang, C., Cerioti, G., Tour, J.M., 2013. Large flake graphene oxide fiberswith unconventional 100% knot efficiency and highly aligned small flake graphene oxide fibers. Adv. Mater. 25 (23), 4592–4597.
Xiaoming, Fang, Ma, Tingli, Guo qing Guan, Morito Akiyama, Tetsya Kida, Eiichi Abe, 2004. Effect of the thickness of the pt film coated on a counter electro de on the p erformance of a dye-sensitized solar cell. J. Electroanal. Chem. 570 (2), 257–263.
Xu, Y., Shi, G., Duan, X., 2015. Selfassembled three-dimensional graphene macro-structures: synthesis and applications insupercapacitors. Acc. Chem. Res. 48, 1666–1675.
Xu, Z., Sun, H., Zhao, X., Gao, C., 2013. Ultrastrong fibers assembled from giant graphene oxide sheets. Adv. Mater. 25 (2), 188–193.
Yan, X., Li, B., Cui, X., Li, L.S., 2010. Large solution- processable grapheme quantum dots as light absorber for photovotalics. Nano Lett. 10 (5), 1869–1873.
Yang, N., 2017. The Preparation ofNano Compositesand TheirApplications in SolarEnergy Conversion. Springer, Verlag, Germany.
Yang, N., Zhai, J., Wang, D., Chen, Y., Jiang, L., 2010. Two-Dimensional Graphene Bridges Enhanced Photoinduced Charge Transport in Dye-Sensitized Solar Cells. ACS Nano 4 (2), 887–894.

Yen, M.Y., Teng, C.C., Hsiao, M.C., et al., 2011. Platinum nano particles/graphene composite catalyst as a novel composite counter electrode for high performance dye sensitized solar cells. Journal of material chemistry 21 (34), 12880–12888.
Yu, Q., Lian, J., Siriponglert, S., Li, H., Chen, Y.P., Pei, S., 2008. Graphene segregated on Ni surfaces and transferredto insulators. Appl. Phys. Lett. 93, 113103.
Yum, J.H., Baranoff, E., Wenger, S., Nazeeruddin, M.K., Gratzel, M., 2011. Panchromatic engineering for dye-sensitized solar cells. Energy Environ. Sci. 4 (3), 842–857.
Ze, Yu., Vlachopoulos, Nick, Gorlov, Mikhail, Kloo, Lars, 2011. Liquid electrolytes for dye-sensitized solar cells. Dalton Trans. 40 (40), 10289–10303.
Zhang, D., Li, X., Chen, S., Sun, Z., Yin, X.J., Huang, S., 2011. Performance of dye-sensitized solar cells with various carbon nanotube counter electrodes. Microchim. Acta 174 (1–2), 73–79.
Zhang, Y., Li, H., Kuo, L., Dong, P., Yan, F., 2015. Recent Applications of Graphene in Dye-Sensitized Solar Cells. Curr. Opin. Colloid Interface Sci. 20 (5–6), 406–415. https://doi.org/10.1016/j.cocis.2015.11.002.
Zhang, R., Li, X., 2018. Multidimensional Assemblies of Graphene. In: Zhu, H., Xu, Z., Xie, D., Fang, Y. (Eds.), Graphene: Fabrication, Characterizations, Properties and Applications. Academic Press, London, United Kingdom, pp. 27–72.
Zhang, L., Shi, G., 2011. Preparation of highly conductive graphene hydrogels for fabricating supercapacitorswith high rate capability. The Journal of Physical Chemistry C 115 (34), 17206–17212.
Zhang, R., Cao, Y., Li, P., Zang, X., Sun, P., Wang, K., Zhu, H., 2014. Three-dimensional porous graphene spongesassembled with the combination of surfactant and freeze-drying. Nano Res. 7 (10), 1477–1487.
Zhao, B., Zhao, J.M., Zhang, Z.M., 2015. Resonance enhanced absorption in a graphene monolayer using deep metal gratings. J. Opt. Soc. Am. B 32, 1176–1185.
Zhen, Z., Zhu, H., 2018. Structure and Properties of Graphene. In: Zhu, H., Xu, Z., Xie, D., Fang, Y. (Eds.), Graphene: Fabrication, Characterizations, Properties and Applications. Academic Press, London, United Kingdom, pp. 1–12.
Zheng, Q., Kim, J.-K., 2015. Graphene for Transparent Conductors: Synthesis, Properties, and Applications. Springer. Synthesis, Structure and Properties of Graphene and Graphene Oxide, New York, pp. 29–94.
Zheng, H., Neo, C.Y., Mei, X., Qiu, J., Ouyang, J., 2012. J. Mater. Chem. 22, 14465.
Zhu, B.L., Liua, F., Li, K., Lv, K., Wu, J., Gan, Z.H., Liu, J., Zeng, D.W., Xie, C.S., 2017. Sputtering deposition of transparent conductive F-doped SnO2 (FTO) thin films in hydrogen-containing atmosphere. Ceram. Int. 43, 10288–10298.
Zhu, G., Xu, T., Lv, T., Pan, L., Zhao, Q., 2011. Graphene-incorporated nanocrystalline TiO2 films for CdS quantum dot-sensitized solar cells. J. Electroanal. Chem. 650, 248.
Zou, J., Kim, F., 2012. Self-Assembly of Two-Dimensional Nanosheets Induced by Interfacial Polyionic Complexation. ACS Nano 6 (12), 10606–10613. https://doi.org/10.1021/nn303608g.